TITLE

High-throughput genetic mapping discovers novel zinc toxicity response loci in *Drosophila melanogaster*

AUTHORS & AFFILIATIONS

Katherine M. Hanson[1], Anthony D. Long[2], and Stuart J. Macdonald[1]

[1] Department of Molecular Biosciences and Center for Genomics, University of Kansas, 1200 Sunnyside Avenue, Lawrence, KS 66045, USA

[2] Department of Ecology and Evolutionary Biology, University of California at Irvine, Irvine, CA 92697, USA

CORRESPONDING AUTHOR INFORMATION

Stuart Macdonald
Department of Molecular Biosciences
University of Kansas
1200 Sunnyside Avenue
Lawrence
KS 66045

Tel: (785) 864-5362
Email: sjmac@ku.edu

KEYWORDS

Extreme QTL mapping; bulked phenotyping; zinc toxicity; DSPR

ARTICLE SUMMARY (80 words)

Starting with an outbred *Drosophila melanogaster* population we repeatedly selected for groups of individuals showing high resistance to toxic levels of zinc during development. Pooled sequencing of these groups, along with matched groups of control individuals, enabled the identification of seven genomic regions – or QTL – contributing to zinc toxicity resistance. Midgut-specific RNAi of genes implicated by these QTL yielded ten genes impacting developmental traits in zinc-supplemented media, including *MTF-1* (a metal response transcription factor) and *pHCl-2* (a zinc sensor protein).

ABSTRACT (247 words)

Heavy metals are a widespread environmental contaminant, and even low levels of some metals can disrupt cellular processes and result in DNA damage. However, the consequences of metal exposure are variable among individuals, with susceptibility to metal toxicity representing a complex trait influenced by genetic and non-genetic factors. To uncover toxicity response genes, and better understand responses to metal toxicity, we sought to dissect resistance to zinc, a metal required for normal cellular function, which can be toxic at high doses. To facilitate efficient, powerful discovery of Quantitative Trait Loci (QTL) we employed extreme, or X-QTL mapping, leveraging a multiparental, recombinant *Drosophila melanogaster* population. Our approach involved bulk selection of zinc-resistant individuals, sequencing several replicate pools of selected and control animals, and identified QTL as genomic positions showing consistent allele frequency shifts between treatments. We successfully identified seven regions segregating for resistance/susceptibility alleles, and implicated several strong candidate genes. Phenotypic characterization of populations derived from selected or control animals revealed that our selection procedure resulted in greater egg-to-adult emergence, and a reduced developmental delay on zinc media. We subsequently measured emergence and development time for a series of midgut-specific RNAi gene knockdowns and matched genetic controls raised in both zinc-supplemented and normal media. This identified ten genes with significant genotype-by-treatment effects, including *pHCl-2*, which encodes a zinc sensor protein. Our work highlights recognized and novel contributors to zinc toxicity resistance in flies, and provides a pathway to a broader understanding of the biological impact of metal toxicity.

INTRODUCTION

Human exposure to toxic levels of various heavy metals has risen due to environmental contamination resulting from mining operations, and the broad use of metal compounds in a range of agricultural and industrial sectors (Jaishankar et al., 2014; Karri et al., 2016; Kim et al., 2019; Rehman et al., 2018; Tchounwou et al., 2012). Exposure to heavy metals primarily occurs through ingestion of contaminated water or food grown in contaminated soil, but can additionally occur via inhalation (Rehman et al., 2018; Tchounwou et al., 2012). Exposure to a high level of heavy metals can harm cells by inducing the production of reactive oxygen species which can damage DNA through oxidative stress, alter the balance of essential elements (for instance, where lead ions can replace iron ions), and affect enzymatic activity (Fu & Xi, 2020; Jaishankar et al., 2014; Rehman et al., 2018). Such metal-induced change can yield severe health consequences, increasing the risk for cancer, cognitive dysfunction, and organ damage (Goutam Mukherjee et al., 2022; Karri et al., 2016; Rehman et al., 2018; Tchounwou et al., 2012). Given the pervasive negative consequences of heavy metal exposure, it is critical to understand how organisms physiologically respond to metal ingestion, and the molecular pathways that are involved.

Although many heavy metals – for instance, cadmium and lead – have no physiological role, metals such as copper, iron, manganese, and zinc are essential heavy metals required for a plethora of biological functions (Kim et al., 2019; Tchounwou et al., 2012). Zinc is abundant in living organisms, has a variety of roles as both a structural and catalytic component of proteins (Kambe et al., 2015), is involved in cell signaling (Fukada et al., 2011), and is estimated to be able to bind to 10% of the human proteome (Andreini et al., 2006). Given its key role in many processes, maintaining an appropriate cellular level of zinc is critical for many biological functions: Zinc deficiency can lead to a range of health problems (Fischer Walker et al., 2009; Prasad, 2013), and conversely excess consumption of zinc – such as the overuse of zinc dietary supplements (Irving et al., 2003; Willis et al., 2005), denture cream (Lasater, 2017; Willis et al., 2005), or inhaling zinc-containing fumes from industrial process such as welding (ATSDR, 2005; Cooper, 2008; Noel & Ruthman, 1988) – can lead to toxicity.

Toxic levels of zinc can induce oxidative stress, inhibit mitochondrial function leading to reduced ATP levels, and induce cell death (Lemire et al., 2008; Maret, 2008; Sensi et al., 2009). Additionally, an important consequence of zinc toxicity is copper deficiency whose symptoms include anemia, leukopenia and neutropenia (Agnew & Slesinger, 2020; Hoffman et al., 1988; Willis et al., 2005). This reduction in copper level is likely due to the high levels of zinc inducing the expression of metallothionein (MT) proteins (a protein family important in metal detoxification), which have a greater affinity for copper than for zinc, resulting in lower levels of free copper (Agnew & Slesinger, 2020; Harold, 2014; Navarro & Schneuwly, 2017; Yiwen et al., 2022).

Central to zinc homeostasis is *MTF-1* (*metal transcription factor 1*), a zinc-sensing transcription factor. When cellular zinc levels are high, MTF-1 will increase the expression of genes regulated by the metal response element enhancer (Andrews, 2001; Stuart et al., 1985; B. Zhang et al., 2001). Such genes include MTs (Egli et al., 2003; B. Zhang et al., 2001), along with some transporters belonging to the zinc transporter (ZnT) family (Guo et al., 2010; Langmade et al., 2000; Yepiskoposyan et al., 2006) which are responsible for transporting cytosolic zinc out to the extracellular matrix or into intracellular compartments. Additionally, MTF-1 will repress

expression of some proteins belonging to the zinc import protein (ZIP) family (Lichten et al., 2011; Zheng et al., 2008) which are responsible for importing zinc into the cytosol.

Many of the proteins that regulate zinc are evolutionarily conserved between mammals and *Drosophila melanogaster* (Lye et al., 2012; B. Zhang et al., 2001), making flies an excellent model to study zinc homeostasis and toxicity. For example, adding the human MTF-1 sequence into *MTF-1* null *Drosophila* cell lines rescues sensitivity to heavy metals, while the *Drosophila* version of MTF-1 is able to rescue sensitivity in MTF-1 knockout mouse cells (Balamurugan et al., 2004). Additionally, the *Drosophila* genome encodes 7 ZnT proteins and 10 ZIP proteins that are homologous to mammalian transporters (Calap-Quintana et al., 2017; Xiao & Zhou, 2016), and flies also possess 6 MTs which help protect against metal toxicity (Luo et al., 2020).

A great deal has been learned about the biological roles of zinc, and the genes, pathways, and mechanisms involved in maintaining zinc homeostasis and avoiding toxicity, from functional studies in whole animals that rely on gene knockouts (Egli et al., 2003; Palmiter & Findley, 1995; Yepiskoposyan et al., 2006), RNAi-based gene expression knockdowns (Lye et al., 2012; B. Zhang et al., 2001), or overexpression of critical genes (Gaither & Eide, 2001; Lye et al., 2012), as well as from cell-based functional genomic screens (Mohr et al., 2018). However, such studies typically employ an esoteric (and often limited) set of genetic backgrounds, which might make inferring the impact of mutations difficult to generalize (Chandler et al., 2013; Sittig et al., 2016). Since there is population-level variation for responses to the toxic effects of heavy metals in general (Evans et al., 2018; Warrington et al., 2015; Xenakis et al., 2022; Zhou et al., 2017), and zinc specifically (Evans et al., 2020), isolating and characterizing loci that segregate for allelic variation impacting susceptibility is a complementary route to understanding zinc biology. For instance, studies in rice (J. Zhang et al., 2017), *Arabidopsis helleri* (Willems et al., 2007), and *Caenorhabditis elegans* (Evans et al., 2020) have isolated QTL (Quantitative Trait Loci) that contribute to variation in zinc resistance, and have led to the identification of novel loci underlying metal resistance/susceptibility.

Here we seek to further understand the biology of zinc homeostasis and toxicity by genetically dissecting variation in zinc resistance using *D. melanogaster*. We take advantage of the "extreme QTL" or X-QTL mapping framework that is an elaboration of bulked segregant analysis (Michelmore et al., 1991). Initially employed in yeast (Ehrenreich et al., 2010), X-QTL mapping starts with a large recombinant population and bulk selects for a phenotype of interest. Individuals who pass the selection threshold – in the present case, adults that emerge from embryos raised through media containing a high level of zinc – are pooled, sequenced, and compared to a pool of non-selected, control animals. QTL are identified as genomic positions showing consistent differences in allele frequency between several replicate pairs of selected and control pools. The X-QTL design we employ extends the approach by starting from a highly-recombinant, outbred multiparental base population derived from the *Drosophila* Synthetic Population Resource (DSPR) (King, Merkes, et al., 2012) and enables powerful QTL mapping, and excellent mapping resolution (Macdonald et al., 2022). The X-QTL approach is particularly amenable to dissecting toxicity traits since bulk phenotypic selection for such traits is straightforward and can be very efficient. For instance, we have successfully used X-QTL mapping to identify loci underlying resistance to caffeine (Macdonald et al., 2022) and the insecticide malathion (Macdonald & Long, 2022). Although these previous experiments discovered novel QTL associated with trait variation, simulations suggest power was limited by a lack of replication and the modest numbers of individuals assayed (Macdonald et al., 2022). Therefore, in the present study we employed 12 experimental replicates, testing tens of

166 thousands of individuals, allowing us to isolate 7 QTL that impact developmental zinc
167 resistance. Follow-up midgut RNAi of a subset of genes within QTL intervals implicated several
168 candidates in the control of trait variation, some of which represent novel contributors to zinc
169 toxicity tolerance in flies, including *pHCl-2* (pH-sensitive chloride channel 2) and *Ndae1* (Na^+-
170 driven anion exchanger 1).

171 MATERIALS & METHODS
172
173 **X-QTL base population:** We employed the same DSPR-derived base population used in two
174 previous X-QTL studies (Macdonald et al., 2022; Macdonald & Long, 2022). Briefly, the DSPR is
175 a set of multiparental advanced generation intercross RILs (Recombinant Inbred Lines) derived
176 from 8 inbred founder strains (King, Merkes, et al., 2012). We collected 10 eggs from each of
177 663 DSPR population A RILs, raised them in standard *Drosophila* media bottles, and placed
178 adult progeny in a population cage. The population was provisioned weekly with fresh media in
179 bottles, and maintained for 64 weeks before egg collection for the first replicate of the zinc
180 selection X-QTL assay (see below). Assuming the population experienced one generation every
181 two weeks, we estimate that the 12 X-QTL replicates were executed 31-36 generations
182 following base population founding.
183
184 **Zinc selection X-QTL assay:** Each of the 12 replicates of the zinc selection assay was
185 executed as follows. Several apple juice agar plates, each holding a small amount of live yeast
186 paste in the center, were placed in the base population cage for ~24-hours. Subsequently,
187 plates were filled with 1X phosphate-buffered saline (PBS), eggs were gently displaced from the
188 plate surface with a paintbrush, and the egg suspension poured into a 50-ml conical tube. Eggs
189 were rinsed with 1X PBS to remove any media residue, and the majority of the 1X PBS drained
190 from the clean eggs, leaving them just submerged. We then pipetted eggs into a series of 6-oz
191 *Drosophila* bottles (Fisher Scientific, AS-355) using a wide-bore pipette tip. The media in each
192 bottle contained 9-g Instant *Drosophila* Medium (Carolina Biological Supply Company, Formula
193 4-24) reconstituted with 40-ml of either water or a 25-mM zinc chloride solution ($ZnCl_2$, CAS
194 Number 7646-85-7, Millipore-Sigma, 793523). We pipetted 24-μl eggs into each water bottle
195 (the non-selection, control treatment), and 48-μl eggs into each zinc bottle (the selection
196 treatment). The greater number of embryos per zinc bottle limited the total number of bottles
197 required, while the larval/adult density per bottle remained low given the toxicity of the zinc
198 chloride concentration employed. For each replicate, we set up four water control bottles and
199 between 8 and 21 zinc bottles (see Supplementary Table 1).
200
201 Bottles were checked for emerged adults every 1-2 days. Flies emerged from the water bottles
202 on days 10-15 following setup, while they emerged from the zinc bottles on days 15-22 due to
203 the developmental delay caused by the zinc treatment. Emerged adults were counted,
204 separated by sex and treatment, and females were frozen at –20°C for subsequent DNA
205 isolation. For replicates R9 and R10, flies were not immediately frozen, and instead were
206 allowed to lay eggs to derive subpopulations to enable a more detailed examination of the
207 phenotypic effects of selection (see below).
208
209 **Pooled DNA isolation:** We routinely collected more non-selected, control females from the
210 water bottles than selected females from the zinc bottles. To maintain the same pool size for the
211 two treatments within each replicate we randomly chose a subset of the non-selected, control
212 females to match the actual number of zinc-selected females that emerged. For five replicates
213 (R5, R6, R8, R11, R12) we had enough control females to generate two independent control
214 pools, enabling a direct examination of variation among pools of control animals. Each of the
215 resulting 29 pools of flies were homogenized in bulk, and DNA was isolated from each using the
216 Puregene Cell Kit (Qiagen, 158046) with a modified protocol (Supplementary Text 1).
217 Resuspended DNA was quantified using a Qubit fluorometer (ThermoFisher).
218

DNA library preparation and sequencing: Each of the 29 pooled DNA samples was diluted to 450-ng in 30-μl, and libraries were constructed following the Illumina DNA Prep protocol (Illumina, 20018705) with unique dual indices (Illumina, 20027213). The 29 libraries ranged in fragment size from 403-bp to 577-bp (Agilent TapeStation 4150), were pooled at equal concentrations, and sequenced with PE150 reads on an Illumina NovaSeq 6000 SP flowcell at the University of Kansas Medical Center Genome Sequencing Facility.

Haplotype estimation and QTL identification: QTL were identified following a similar framework as used in a previous X-QTL study employing the same base population (Macdonald & Long, 2022). Briefly, raw reads from each of the 29 X-QTL samples, along with reads from the founder strains of DSPR population A (King, Merkes, et al., 2012), were mapped to Release 6 (dm6) of the *D. melanogaster* reference genome with bwa-mem (Li, 2013). We used bcftools (Li, 2011) to obtain REF and ALT counts for every SNP, and these were converted to REF allele frequencies at each SNP for each sample. We subsequently moved along the genome in overlapping 1.5-cM windows, and for each window for each X-QTL sample used the R/limSolve package (Soetaert et al., 2009) to estimate the founder haplotype frequencies based on the observed SNP frequencies in the X-QTL sample, and the known founder haplotypes. For additional detail of the method, along with validation of the accuracy of this estimation approach, see both Linder et al. 2020 and Macdonald et al. 2022.

The estimated founder haplotype frequencies for each replicate and treatment were arcsine square-root transformed (ASF), then tested for differentiation between treatments using an ANOVA ($ASF \sim Treatment + Haplotype + Treatment \times Haplotype$). For each window we calculated a $-\log_{10}(P)$ value by testing the $Treatment \times Haplotype$ interaction term against $Replicate \times Treatment \times Haplotype$ as the error term. Subsequently we LOESS smoothed the genomewide set of $-\log_{10}(P)$ values to compensate for window-to-window variation, identified QTL peaks as those positions exceeding a significance threshold of $-\log_{10}(P) = 4$, and for each peak identified the confidence interval on location as a 3 $-\log_{10}(P)$ drop confidence interval.

Phenotypic consequences of selection for increased developmental zinc resistance: We generated several populations/strains, and executed several experiments to examine the phenotypic impact of zinc exposure during development.

Deriving subpopulations from emerged X-QTL animals: For replicates R9 and R10 of the X-QTL study, we collected all emerging flies from the two treatment regimes as living animals. All those adults emerging from the zinc-selection treatment for a given replicate were split among several vials containing cornmeal-yeast-molasses media, and allowed to lay eggs for 72 hours. Flies emerging from the non-selected, water control treatment were treated similarly, except we only used a random subset of the animals to match the (lower) number of animals emerging from the zinc selection treatment. The four subpopulations – R9C, R9Z, R10C, R10Z (where “C” and “Z” represent the control and zinc treatments, respectively) – were maintained in sets of vials for several generations and used for phenotyping (below).

Generating lines from X-QTL subpopulations: In an effort to stabilize the genotypes of the outbred subpopulations, following seven generations of subpopulation maintenance, we established 22 lines from R9C (R9C-lines) and 23 from R9Z (R9Z-lines) using single, mated females from the subpopulations, and followed this with 6-8 generations of inbreeding (crosses between a single virgin female and one male). Clearly these lines are only partially inbred, and to reflect this we refer to them as “semi-inbred lines” throughout.

Establishing new DSPR-derived cohorts of zinc-selected and control animals: Part way through the project we disposed of the X-QTL base population. To continue our phenotypic testing, we derived a new population by collecting 10 eggs from each of 83 DSPR population A RILs, allowing the population to mix/recombine for five generations. Next, we collected eggs and followed the same protocol described above (see the "Zinc selection X-QTL assay" section) yielding cohorts of zinc-selected and non-selected, control animals. These groups were allowed to mate and lay eggs, were maintained for two generations, and then were tested in phenotypic assays (see below). We refer to these as the selected and non-selected phenotyping-only test cohorts.

Assaying developmental resistance to heavy metals: Test vials contained 50 eggs on media containing 1.8-g Instant *Drosophila* Medium mixed with either 8-ml of water or a heavy metal salt solution. We used solutions of zinc chloride (10- or 25-mM depending on the experiment), 2-mM copper sulfate ($CuSO_4$, CAS number 7758-98-7, Millipore-Sigma, C1297), and 0.2-mM cadmium chloride ($CdCl_2$, CAS number 10108-64-2, Millipore-Sigma, 655198). Emerged flies were sexed/counted up to 30 days following egg collection. We calculated the fraction of adults emerging per vial, and the egg-to-adult development time (in days) for every individual emerged adult.

We assayed developmental zinc resistance in all four subpopulations derived from replicates R9 and R10 of the X-QTL study (R9C, R9Z, R10C, R10Z) by testing 10 25-mM $ZnCl_2$ vials and 2-3 water vials per subpopulation. The two sets of semi-inbred lines (the R9C- and R9Z-lines) were tested for developmental resistance to a lower concentration of zinc (~3 10-mM $ZnCl_2$ vials per line, and 63-68 per set), copper (1 vial/line, 22-23 vials/set), and cadmium (1 vial/line, 22-23 vials/set), with water controls (1 vial/line, 22-23 vials/set). We were forced to reduce the test $ZnCl_2$ concentration to 10-mM given that pilot work showed most semi-inbred lines had zero emergence at 25-mM $ZnCl_2$. Finally, we tested eggs from the selected and non-selected phenotyping-only test cohorts for resistance to zinc (40 25-mM $ZnCl_2$ vials per cohort), copper (40 vials per cohort), and cadmium (40 vials per cohort), along with 38-39 water vials per cohort.

Measuring zinc resistance in adults: Assays were carried out in standard narrow fly vials containing 1.8-g Instant *Drosophila* Medium with 8-ml of either water or 100-mM $ZnCl_2$. Twenty 2-6 day old, likely mated females were placed into each vial, and dead flies were counted daily until day 7 (by this point all flies in the zinc-containing vials had died). Flies in water-control vials were moved to fresh vials every 2-3 days to maintain media quality (given the absence of a toxic level of zinc, the action of larvae made the instant media wet/sticky). We assayed adult zinc resistance in the four X-QTL subpopulations (R9Z, R9C, R10Z, R10C) over two batches, using 10 zinc and 2 water vials per subpopulation in batch 1, and 20 zinc and 2 water vials per subpopulation in batch 2. We also assayed 25 zinc vials and 6 water vials for each of the selected and non-selected phenotyping-only test cohorts.

Testing X-QTL candidate genes via RNAi: Collectively, the X-QTL intervals we resolved contain several hundred protein-coding genes. Candidate genes for RNAi testing were prioritized using the following information. First, we identified those genes known to be involved in zinc homeostasis (i.e., *MTF-1*, and any members of the MT, ZnT or ZIP families). Second, we examined FlyBase (release FB2022_03) information associated with each gene (Gramates et al., 2022), particularly focusing on genes associated with the gene ontology (GO) terms zinc ion binding (GO:0008270), intracellular zinc homeostasis (GO:0006882), response to oxidative

stress (GO:0006979), as well as other terms related to zinc and other essential metals (i.e., magnesium, copper, cadmium, and iron). Third, we cross-referenced genes under our mapped QTL with genes identified in a cell-based RNAi screen for zinc toxicity modifiers, and those that showed a significant transcriptional change in response to zinc exposure (Mohr et al., 2018, see their File S1 and S2 datasets). Fourth, we marked genes found in previous metal toxicity studies and relevant review articles (Navarro & Schneuwly, 2017; Redhai et al., 2020). Collectively, we identified 24 candidate genes within our mapped QTL (Supplementary Table 2). We note that ongoing optimization of our X-QTL mapping routines throughout this project led to slight differences in the locations of QTL boundaries between the time we evaluated candidate genes, and the time of writing, so 3/24 candidates are just outside of the X-QTL boundaries we report here (Table 1, Supplementary Table 2).

We knocked down candidate genes using the X-linked *mex1*-GAL4 driver (Bloomington *Drosophila* Stock Center, BDSC 91367), which is reported to express GAL4 in the middle midgut from embryos through to second instar larvae (Phillips & Thomas, 2006). All UAS-RNAi and control stocks were derived from the Transgenic RNAi Project (TRiP) resource (Perkins et al., 2015). We used the following 4 control strains: UAS-GFP (BDSC 35786), UAS-Luciferase (35788), empty attP2 docking site (36303), and an empty attP40 docking site (36304). The following UAS-RNAi lines were used to successfully test 18 candidate genes: *ATPsynD* (33740), *bendless* (28721), *CG11318* (51792), *CG4496* (51428), *dj-1β* (38999), *GluRIB* (67843), *Hsp22* (41709, which will also impact expression of the overlapping gene *CG4456*), *Mekk1* (28587), *Mnn1* (51862), *MTF-1* (33381 and 34094), *Ndae1* (62177), *Ndc1* (67275), *Nup98-96* (28562), *Octα2R* (50678), *pHCl-2* (26003), *RanBP3* (40948), *Trpm* (51713 and 57871), and *Xrp1* (34521 and 51054). Initial tests of RNAi for two candidate genes – *Fer1HCH* (60000) and *Fer2LCH* (44067) – revealed almost no adult GAL4:UAS-RNAi flies emerging on control media, suggesting knockdown of these genes via *mex1*-GAL4 leads to lethality in the absence of zinc supplementation; we did not pursue these genes further. Finally, we did not test four of our candidate genes – *Gart*, *Vha36-1*, *Vha14-1*, *CG14302* – since TRiP RNAi lines were not available.

Virgin female *mex1*-GAL4 females were crossed to males from the RNAi control and UAS-RNAi strains, avoiding balancer-containing males for those strains segregating for a balancer chromosome. After the first day of mating in standard media vials, crosses were tipped into custom egg laying chambers. Each chamber is constructed from a polypropylene fly vial (Fisher Scientific, AS507) with the base removed and replaced with a cotton ball. Flies are enclosed in the chamber by capping it with a polyethylene flanged plastic cap (MOCAP, FCS13/16NA1) containing ~4.5-ml of cornmeal-yeast-molasses media plus a small amount of live yeast paste to encourage egg laying. Media caps were replaced daily for 4 days, and each day eggs were collected manually. Eggs were placed in groups of 50 into water-control or 10-mM $ZnCl_2$ treatment vials (standard narrow fly vials containing 1.8-g Instant *Drosophila* Medium reconstituted with 8-ml of solution). Following egg collection, we sexed/counted emerged flies for 30 days. Five batches of the experiment were completed, resulting in 17-21 replicate vials per treatment per candidate gene RNAi, and 28-29 replicate vials per treatment for each RNAi control genotype. As for the phenotyping populations and strains (above) we measured adult emergence on a per-vial basis, while egg-to-adult development time was assessed for every emerging adult in days.

364 We note that the RNAi experiment used a lower $ZnCl_2$ concentration than our X-QTL experiment
365 (10-mM *versus* 25-mM); This was enforced by pilot RNAi experiments using the higher
366 concentration, during which no eggs developed into adults.
367
368 **Fly maintenance:** Aside from the X-QTL base population and the second population created
369 from 83 RILs, (which were both maintained in population cages at normal laboratory conditions),
370 all flies were reared/tested in an incubator at 25°C, 50% humidity, with a 12-hour dark:light
371 cycle. For normal development/maintenance, all populations and strains were maintained using
372 a cornmeal-yeast-molasses media (see Supplementary Text 2).
373
374 **Data availability:** The DSPR RILs used in the construction of the X-QTL base population are
375 available from the BDSC. Raw X-QTL sample FASTQ sequencing data is available from the
376 NCBI SRA under accession number PRJNA1127662. All summary information and statistical
377 results are presented in supplementary files accompanying this work, and all analysis code is
378 available on GitHub (https://github.com/Hanson19/Zinc-X-QTL).

379 RESULTS
380
381 **Discovery of zinc toxicity resistance loci:** We established an outbred base population by
382 mixing together animals from >600 8-way population A DSPR RILs (King, Macdonald, et al.,
383 2012) resulting in a population that segregates for the 8 DSPR founder haplotypes at any given
384 genomic position. We then created a developmental zinc toxicity assay that can be easily
385 carried out in bulk at large scale, and selected animals with genotypes that confer relatively
386 greater resistance to zinc. Over 12 replicates of this X-QTL design, eggs were collected from
387 the base population, and allowed to develop to adulthood on either a non-selection, control
388 treatment media or a selection treatment media containing 25mM $ZnCl_2$. We did not count the
389 number of embryos tested, but based on the number of flies emerging from the non-selection,
390 control treatment, we estimate that each replicate tested around 4,300 female embryos on the
391 zinc treatment (range = 2,600-6,000), and that ~7% of these survived to adulthood
392 (Supplementary Table 1). For each replicate, we isolated DNA from a pool of all females
393 emerging from the zinc treatment, and a pool of an equivalent number of females coming from
394 the non-selection, control treatment, and sequenced each pool to an average of ~67X coverage.
395
396 Following read alignment and SNP calling, we moved through the genome in windows, and for
397 each X-QTL sample estimated the frequency of the 8 DSPR founder haplotypes in that window.
398 QTL are then detected as consistent, significant shifts in the founder haplotype frequencies
399 between the non-selected, control samples and the zinc selection samples (see "Materials &
400 Methods" for additional detail). We employed $-\log_{10}(P)=4$ as our significance threshold since our
401 previous work showed this led to a genomewide false positive detection rate at or below 5%
402 (Macdonald et al., 2022). Additionally, by directly comparing the five pairs of duplicate non-
403 selection, control treatment pools (taken from replicates R5, R6, R8, R11, and R12) we see
404 limited evidence for allele frequency shifts between duplicates, and no peaks reaching
405 $-\log_{10}(P)=4$ (Supplementary Figure 1). This suggests our haplotype frequency estimates are
406 accurate, and peaks above $-\log_{10}(P)=4$ likely represent true causative factors impacting zinc
407 resistance.
408
409 We identified 7 peaks – QTL-A to QTL-G – above our significance threshold of $-\log_{10}(P)=4$ that
410 are in regions of normal recombination, and these are spread across the genome on all major
411 chromosome arms (Figure 1, Table 1). None of the QTL overlap with intervals implicated by our
412 previous work on adult caffeine and malathion insecticide resistance using the same base
413 population (Macdonald et al., 2022; Macdonald & Long, 2022). QTL-E does colocalize with a
414 QTL previously identified for development viability in the presence of 2-mM copper identified
415 using a subset of the DSPR population B RILs (Everman et al., 2021). However, we cannot
416 know if this pair of QTL are driven by the same molecular factor since the mapping results
417 derive from genetically distinct populations; the base population we use here is derived from the
418 DSPR A RILs, and the A and B RILs were founded with different sets of strains (King, Merkes,
419 et al., 2012).
420
421 These 7 QTL implicate intervals of 300-1250 Kb, with the majority being less than 1000-Kb
422 (Table 1). These intervals are smaller than in our previous DSPR-based X-QTL studies
423 (Macdonald et al., 2022; Macdonald & Long, 2022) since we execute a greater number of
424 experimental replicates (12 *versus* 4), which yields greater mapping power and resolution
425 (Macdonald et al., 2022). Collectively, 631 protein-coding genes reside within our 7 QTL, and 5
426 QTL harbor fewer than 90 such genes. We note that our X-QTL genome scan also revealed
427 evidence for peaks in the centromeric regions of chromosomes 2 and 3 (Figure 1). These peaks

428 are physically large (2.3-5.5 Mb) since they implicate areas of reduced recombination, making
429 identifying causative candidate genes extremely difficult. Thus, we focused on the 7 QTL peaks
430 identified in regions of normal recombination.
431
432 **Haplotype frequency changes due to zinc selection at mapped QTL:** Since QTL are
433 identified as significant shifts in founder haplotype frequency due to the zinc exposure
434 treatment, we can identify founders that possess resistant or susceptible alleles as those
435 showing an increase or a decrease in frequency relative to controls. Figure 2 illustrates the
436 change in founder haplotype frequency at each of the 7 peaks, showing it is routinely the case
437 that the frequencies of only 1-2 haplotypes change substantially between the zinc and control
438 treatments. A possible interpretation is that the functional alleles mapped via X-QTL are
439 relatively rare, with "extreme" alleles present in just one or two founders. However, at each of
440 the QTL we identify here, the founder haplotypes showing substantial change in frequency due
441 to treatment are always at high frequency in the non-selection, control pools (Supplementary
442 Figure 2). Indeed, for every one of our QTL, the frequency of the most common 1-2 founders in
443 the control pools sums to nearly 50%.
444
445 Unlike some other multiparental mapping panels, the DSPR RILs that we mixed to create the
446 outbred base population exhibit considerable heterogeneity in founder haplotype frequencies
447 along the genome, with a great deal of variation away from the 1/8 (12.5%) frequency expected
448 (compare Figures 3-4 from Collaborative Cross Consortium, 2012 to Figure 2 from King, Merkes
449 et al., 2012). This pattern is likely due the actions of random genetic drift and selection during
450 the 50 generations of interbreeding that were used to build up recombination events in the
451 populations from which the DSPR RILs were derived. As a result, since some founder
452 haplotypes are at very low frequency at any given position in the DSPR-derived base
453 population, our X-QTL mapping is effectively contrasting fewer than 8 alleles at any given locus.
454 Thus, it is difficult to estimate the frequency of resistant or susceptible alleles in the species as a
455 whole from our data.
456
457 **Evaluating the phenotypic impact of developmental zinc exposure:** Exposure to high levels
458 of $ZnCl_2$ during the X-QTL selection assay resulted in fewer eggs surviving to adulthood (~7%
459 surviving) and an increase in egg-to-adult development time (of ~5 days). To further explore the
460 consequences of our zinc selection regime, we directly examined emergence (the percentage of
461 eggs that develop into adults) and development time (the time, in days, between egg collection
462 and adult emergence), in several different samples of animals derived from zinc selection and
463 control, non-selection treatments: (1) Subpopulations of animals derived from the zinc-selected
464 (Z), and the control, non-selected (C) animals that emerged in replicates R9 and R10 of the X-
465 QTL mapping assay, (2) a series of partially (or semi-) inbred strains derived from the R9Z and
466 R9C cohorts, and (3) animals derived via the same basic selection scheme used for the X-QTL
467 mapping assay, but derived from a distinct base population established with just a fraction of the
468 DSPR RILs, that yielded a pair of test cohorts we only employed for phenotyping. Our goal was
469 to determine whether animals derived from selected and control groups responded differently to
470 zinc treatment.
471
472 *Developmental zinc exposure selects for genotypes with increased emergence on zinc media:*
473 Figure 3 shows the results of experiments examining egg-to-adult emergence on water control
474 and zinc media for the 3 sets of populations described above (see Supplementary Table 3 for
475 full ANOVA analysis results). For animals derived from our X-QTL selected and control, non-
476 selected populations there was no population-by-treatment interaction ($p = 0.17$), potentially

477 because this experiment had few water-control treatment vials (Figure 3A). However, animals
478 from the zinc-selected cohorts did show increased emergence from zinc-containing media (*t*-
479 test, $p < 0.005$, Figure 3A). The semi-inbred lines we constructed from our X-QTL cohorts
480 showed no population-by-treatment interaction ($p = 0.87$, Figure 3B), suggesting that during the
481 course of maintenance/inbreeding the subtle emergence phenotype may have been lost.
482 Finally, the phenotyping-only test cohorts showed a significant population-by-treatment
483 interaction ($p = 0.02$, Figure 3C). Overall, these results suggest that selection via developmental
484 zinc exposure results in populations with increased egg-to-adult emergence on zinc-containing
485 media.
486
487 *Zinc-selected animals exhibit reduced developmental delay on zinc-containing media:* Figure 4
488 presents the egg-to-adult development time results from the same experiments that led to
489 Figure 3. Figure 4A highlights a significant population-by-treatment interaction ($p < 0.0005$, see
490 Supplementary Table 4 for full ANOVA results); development time is similar for both X-QTL
491 subpopulations in water control vials, but zinc-selected populations show shorter development
492 time, i.e., exhibit a reduced developmental delay due to zinc. We see a similar result for the
493 semi-inbred lines that were derived from the X-QTL subpopulations (Figure 4B, population-by-
494 treatment interaction, $p < 10^{-25}$), but see no effect in the phenotyping-only cohorts (Figure 4C),
495 perhaps because relatively few animals emerged from zinc treatment vials in this experiment.
496 Regardless, developmental selection for zinc resistance, in addition to enhancing emergence in
497 zinc conditions (above and Figure 3), appears also to reduce the developmental delay that is a
498 consequence of zinc treatment.
499
500 **Evaluating candidate genes via midgut-specific RNAi knockdowns:** Of the 631 protein-
501 coding genes within our X-QTL intervals, gene ontology information and data from previous fly
502 studies of metal toxicity led us to 24 candidate genes (Supplementary Table 2). We were able to
503 test the effect of 18 of these on developmental zinc resistance using a *mex1*-GAL4 driver which
504 is expressed specifically in the midgut through all three stages of larval development (Binks et
505 al., 2010; Phillips & Thomas, 2006; Tennessen et al., 2011). The midgut is arguably the relevant
506 tissue for our target phenotypes since it is the primary site of nutrient absorption, and is where
507 zinc absorption and homeostasis is primarily mediated (Lemaitre & Miguel-Aliaga, 2013;
508 Navarro & Schneuwly, 2017).
509
510 RNAi knockdown of a gene can impact measured developmental phenotypes in the absence of
511 any zinc challenge. Such events might indicate a gene influences the developmental response
512 to zinc, but we are more interested in those genes that show a change in phenotype in response
513 to a zinc challenge that *differs* between wildtype and knocked down gene expression levels.
514 Analytically this is indicated by a significant interaction between genotype (UAS-RNAi
515 knockdown *versus* wildtype genetic control) and treatment (zinc-containing *versus* water control
516 treatments) and can be visualized by the slope of the lines connecting the mean phenotype on
517 the two treatments for each genotype (see Figure 5).
518
519 We employed multiple wildtype genetic controls to contrast with the UAS-RNAi knockdown
520 genotypes; UAS-GFP and UAS-Luciferase strains express GFP or Luciferase, respectively,
521 under UAS control, as well as strains that simply carry empty attP2 or attP40 docking sites (the
522 positions where the UAS transgene is integrated). After crossing each of these to the *mex1*-
523 GAL4 we saw significant variation in the emergence of progeny on zinc-supplemented media
524 among the control genotypes, with the attP2-containing genotypes showing just 3% emergence
525 on zinc-supplemented media *versus* 15-25% emergence for the other three control genotypes

526 (Supplementary Figure 3, Supplementary Table 5). Given the wide variation among control
527 genotypes, separately for each phenotype – emergence and development time – every RNAi
528 knockdown genotype was contrasted with each of the four control genotypes in a separate full
529 factorial ANOVA. In order to focus on the most interesting gene knockdown effects, RNAi "hits"
530 for a given phenotype were called when the genotype-by-treatment interaction for at least one
531 ANOVA was significant at $p < 0.0003$ (= 0.05/(21 × 4 × 2), since we tested 21 different UAS-
532 RNAi genotypes, against 4 controls, for 2 phenotypes), the interaction was at least nominally
533 significant ($p < 0.05$) for the other three ANOVAs, and the direction of the effect was consistent
534 over the 4 tests.
535
536 We assessed the effect of midgut-specific RNAi-based knockdown for 18 genes using a set of
537 21 UAS-RNAi constructs (3 genes were tested with 2 different constructs). Ten genes emerged
538 as hits. Results are summarized in Table 2 (see Supplementary Table 6 for full results of all
539 analyses), and Figure 5 highlights results for 3 genes we discuss in more depth below (see
540 Supplementary Figure 4 for similar plots for all genes tested). As shown in Table 2, 1 gene
541 impacted only emergence, 7 impacted only development time, and 2 impacted both phenotypes
542 (although for one of these genes – *Xrp1* – the effects on the two phenotypes were seen in
543 different RNAi genotypes). The lack of consistency across the phenotypes implies the
544 underlying genetics of the two traits may be at least partly distinct. Interestingly, our hits are
545 enriched for those where expression knockdown appears to *increase* resistance. This is likely
546 because some of our control, non-knockdown genotypes perform quite poorly on zinc media in
547 our assay (Supplementary Figure 3), and it is therefore difficult for RNAi knockdowns to be
548 statistically worse. We tested at least one candidate gene for each of the 7 mapped X-QTL
549 (Table 1), and 5 QTL showed at least one hit (Table 2).Two of the genes with hits –*MTF-1* and
550 *pHCl-2* – are associated with the "response to metal ion" GO term (GO:0010038), with *pHCl-2*
551 specifically associated with the "cellular response to zinc ion" term (GO:0071294). Additionally,
552 three of our hits – for *GluRIB*, *Ndae1*, and *Nup98-96* – were also hits for $ZnCl_2$ response in a
553 cell-based RNAi screen (Mohr et al., 2018). Notably, for *GluRIB* and *Nup98-96* our results
554 matched observations from this cell-based screen in that knocking down expression of these
555 genes *increases* resistance to zinc.
556
557 **Knockdown of *MTF-1* in the midgut increases egg-to-adult emergence on zinc media:**
558 *MTF-1* encodes a metal transcription factor that, in addition to playing a role in the detoxification
559 of a range of metals, is involved in zinc homeostasis and detoxification, and induces the
560 expression of zinc transporters and metallothionein proteins (Balamurugan et al., 2004; Egli et
561 al., 2003; Navarro & Schneuwly, 2017). We knocked down expression of *MTF-1* using two
562 different UAS-RNAi constructs, and found a significant genotype-by-treatment emergence effect
563 for UAS ID 33381 (Table 2, green line in Figure 5A); compared to all four genetic controls, this
564 *MTF-1* knockdown shows enhanced emergence in media supplemented with zinc. The second
565 UAS (ID 34094) shows the same trend, but the genotype-by-treatment interaction is not
566 significant in all cases (Table 2). There was no evidence for an effect of either *MTF-1*
567 knockdown on development time (Table 2, Figure 5B).
568
569 That knocking down the expression of *MTF-1* results in increased resistance in our study is
570 somewhat counterintuitive since a number of studies have shown that *MTF-1* loss-of-function
571 mutations result in susceptibility to the toxic effects of metals (Bahadorani et al., 2010;
572 Balamurugan et al., 2004; Egli et al., 2003; Wang et al., 2004). This being said, Bahadorani et
573 al. (Bahadorani et al. 2010) showed that while *MTF-1* null flies were more susceptible to
574 cadmium, iron and copper toxicity, nulls showed no difference in zinc susceptibility compared to

wildtype. The same study also showed that overexpression of *MTF-1* made flies more susceptible to zinc exposure both as adults (flies died more quickly) and as larvae (fewer eggs developed into adults), in contrast to the result for other metals, where *MTF-1* overexpression increased resistance. Combined with our results, this work suggests there may be a more complex relationship between zinc toxicity resistance and *MTF-1* expression level.

Reduced *Ndae1* expression results in greater developmental delay in zinc media: *Ndae1* encodes an Na^+-driven anion exchange membrane protein found in the nervous system, throughout the digestive tract, and in the malpighian tubules (Romero et al., 2000; Sciortino et al., 2001). In a RNAi screen using *Drosophila* cultured cells exposed to toxic zinc conditions, *Ndae1* was identified as a high confidence hit whose knockdown led to increased zinc resistance as measured by ATP level, an indirect readout of cell viability (Mohr et al., 2018).

In our tests, the impact of *Ndae1* knockdown on emergence was dependent on the genetic control to which it is compared (Table 2, Figure 5C). However, *Ndae1* knockdowns showed significant genotype-by-treatment effects for development time against all 4 control genotypes (Table 2, Figure 5D), with reduced expression resulting in greater development time in zinc media, i.e., increased susceptibility (see the greater slope of the blue *Ndae1* RNAi line in Figure 5D). This reduction in resistance appears to contradict the observations made by Mohr et al (Mohr et al., 2018). This discrepancy could be the use of different models (whole animals *versus* cultured cells), or different readouts (direct measures of emergence and development time *versus* a proxy for cell viability), and would require additional investigation to understand.

RNAi-based *pHCl-2* expression knockdown results in lower emergence and greater development time in zinc media: *pHCl-2* encodes a zinc-gated chloride channel that is expressed in the midgut, concentrated in the copper cell region (an acid-secreting region of the midgut, sometimes considered the fly “stomach”), and in the malpighian tubules (Feingold et al., 2016; Redhai et al., 2020; Remnant et al., 2016). Previous work suggests that *pHCl-2* is a zinc sensor and that it may play a role in directing larvae to nutrient-rich food (Redhai et al., 2020).

pHCl-2 impacted emergence on zinc media, with the *pHCl-2* midgut-specific knockdown genotype showing greater emergence than controls in zinc conditions (Table 2, Figure 5E), i.e., *pHCl-2* knockdown appears to increase resistance to the toxic effects of zinc. These results mirror data from similar experiments testing *pHCl-2* (known previously as CG11340) gut RNAi knockdown and gene knockouts on media supplemented with copper; *pHCl-2* knockdown/knockout increases survival compared to the control (Remnant et al., 2016). We additionally found significant genotype-by-treatment interactions for development time for all *pHCl-2* RNAi versus genetic control contrasts (Table 2), with the knockdown genotype showing reduced developmental delay in response to zinc media (see lower slope of red line in Figure 5F), again indicating lower expression of *pHCl-2* yields zinc resistance.

615 DISCUSSION
616
617 In this study, we employed an "extreme" or X-QTL mapping approach to identify regions of the
618 genome harboring variants contributing to developmental zinc resistance in *Drosophila*
619 *melanogaster*. We successfully mapped several such QTL across the major *D. melanogaster*
620 chromosome arms, with five of the QTL - all present in euchromatic genomic regions having
621 normal levels of recombination - resolving to relatively modest genomic intervals of 300-820kb,
622 or 0.65-2.85cM (see Table 1). The mapping power and resolution we achieved in the present
623 study is higher than in our previous caffeine resistance X-QTL work (Macdonald et al., 2022),
624 which we attribute both to the greater number of experimental replicates employed (12 versus 4)
625 and the larger number of individuals in the DNA pools (an average of 302 versus an average of
626 245). This highlights the value of increased replication and pool size in X-QTL designs for
627 improving QTL detection and localization, as we previously claimed via simulations (Macdonald
628 et al., 2022).
629
630 **Zinc toxicity resistance represents a multi-faceted phenotype:** Our study suggests that zinc
631 toxicity resistance is a complex trait encompassing multiple components, primarily egg-to-adult
632 viability and development time. However, the nature of resistance appears to extend beyond
633 these two aspects. Through our experiments with different populations/strains, we observed that
634 the components of zinc resistance can be dissociated. For instance, semi-inbred lines derived
635 from zinc-selected populations maintained resistance in terms of developmental time but lost
636 the emergence rate advantage (compare Figures 3B and 4B), possibly due to genetic drift
637 occurring during establishment of the lines. Conversely, the zinc-selected, phenotyping-only
638 cohort showed improved emergence rates on zinc media but no difference in developmental
639 time (compare Figures 3C and 4C). These observations suggest that developmental time and
640 emergence rate under zinc stress are independent phenotypes, a notion further supported by
641 our RNAi results where gene knockdowns could affect either or both phenotypes (see Table 2).
642
643 There also appears to be a distinction between zinc resistance during development and that
644 during adulthood; Adult females from populations that experienced developmental zinc selection
645 showed no increased resistance to zinc, and in some cases even exhibited a slightly higher
646 mortality rate during zinc exposure (Supplementary Figure 5). This underscores the importance
647 of considering life stage-specific responses when studying metal toxicity (Everman et al., 2021).
648 The complexity of zinc resistance is further highlighted by the potential concentration-dependent
649 effects we observed. Our X-QTL mapping used 25mM $ZnCl_2$, while subsequent phenotyping of
650 semi-inbred lines and RNAi knockdowns necessitated a lower concentration of 10mM $ZnCl_2$ due
651 to the extreme toxicity of the higher dose for those. The difference in concentration could
652 contribute to variation in observed phenotypes, and re-emphasizes the importance of
653 considering dose-dependent responses in toxicity studies (Knowles et al., 2018; Wang &
654 Kruglyak 2014; Widmayer et al., 2022). Collectively, our findings suggest zinc toxicity is a
655 complex trait with multiple, potentially independent components that can vary across
656 developmental stages and zinc concentrations.
657
658 **Impact of selection for zinc resistance on susceptibility to other heavy metals:** The zinc
659 resistance loci we identify here do not overlap in location with those previously mapped for
660 caffeine and malathion resistance using the same base population (Macdonald et al., 2022;
661 Macdonald & Long, 2022). With the caveat that we do not have perfect power in any of these
662 studies, this suggests that the genetic basis of zinc resistance is distinct from these other
663 xenobiotic toxicity traits. However, one of the zinc resistance QTL (QTL-E) does colocalize with

664 a locus contributing to copper resistance identified in an independent set of DSPR RILs
665 (Everman et al., 2021), potentially hinting that there are some shared mechanisms of resistance
666 between zinc and copper, two heavy metals, as has been previously suggested in *C. elegans*
667 (Evans et al., 2020).
668
669 To explore the specificity of the zinc resistance in our populations, we tested our semi-inbred
670 lines and phenotyping-only cohorts against toxic concentrations of copper (2mM $CuSO_4$) and
671 cadmium (0.2mM $CdCl_2$) in addition to a zinc challenge. In the semi-inbred lines raised on zinc
672 media, those lines derived from the zinc-selected population exhibit a reduced developmental
673 delay (Figure 4B), but this pattern is not recapitulated when they are raised on copper or
674 cadmium media (Supplementary Figure 7B). In the phenotyping-only cohorts, when raised on
675 zinc media the zinc-selected cohort has a higher rate of emergence than the control cohort
676 (Figure 3C), whereas when raised on cadmium medium the opposite pattern is observed; zinc
677 selection reduces emergence on cadmium media (Supplementary Figure 6A). Additionally,
678 while the zinc-selected and control phenotyping-only cohorts do not differ in development time
679 on zinc media (Figure 4C), the zinc-selected cohorts show slower development on cadmium
680 and copper media than the control cohorts (Supplementary Figure 7A). These results suggest
681 that in some instances the genetic mechanisms underlying zinc resistance may confer
682 susceptibility to other heavy metals.
683
684 Contrasting effects in resistance between zinc and other heavy metals have been documented
685 previously. For example, Bahadorani et al. (2010) found that MTF-1 overexpression had the
686 opposite effect on zinc resistance compared to other heavy metals like cadmium and copper.
687 Such differences may be related to distinct chemical properties of the metals. Zinc is redox
688 neutral in biological systems, unlike copper and iron, and only promotes formation of reactive
689 oxygen species at high, toxic levels (Harold, 2014; Kambe et al., 2015; Maret, 2013; Navarro &
690 Schneuwly, 2017). Metals such as copper may induce toxicity response pathways that our zinc-
691 selected flies may not be adapted to handle effectively. In terms of cadmium, studies in *C.*
692 *elegans* suggest that cadmium toxicity can cause zinc deficiency by activating zinc detoxification
693 pathways (Earley et al., 2021; Moyson et al., 2018; Power & de Pomerai, 1999). Earley et al.
694 (2021) demonstrated that the major pathways governing zinc toxicity resistance are not
695 significantly involved in cadmium resistance. This separation of pathways could explain why our
696 zinc-selected flies are not better equipped to survive cadmium exposure, and may even be
697 more susceptible to zinc deficiency induced by cadmium. Additional studies using our X-QTL
698 design seeking to characterize the genetic basis of variation in susceptibility to a range of
699 metals would enable better examination of metal-specific genetic adaptations.
700
701 **Mapped X-QTL do not routinely harbor known zinc toxicity/homeostasis genes:** Our X-
702 QTL mapping revealed seven loci contributing to zinc toxicity resistance, with only three
703 intervals containing genes previously associated with zinc homeostasis: *Trpm* in QTL-C, *MTF-1*
704 in QTL-D, and *MtnF* in QTL-F. Perhaps surprisingly, most known zinc transporters were not
705 found within our QTL, despite them commonly being focus of zinc toxicity and homeostasis
706 research. One potential explanation is that there is limited functionally-relevant standing
707 variation at such genes, making them harder to detect via our mapping design. Regardless, the
708 observation highlights the potential importance of other gene families in mediating zinc
709 resistance, and underscores the value of unbiased, genome-wide approaches like X-QTL
710 mapping in uncovering novel factors contributing to metal toxicity resistance. Furthermore, by
711 delivering QTL intervals that implicate only a modest number of genes, X-QTL can enable
712 subsequent characterization of novel causative loci.

713
714 **Midgut-specific RNAi knockdowns identify genes important in zinc toxicity, while**
715 **challenging some extant assumptions:** Our RNAi-based functional testing of candidate
716 genes within the QTL intervals yielded several interesting results. We identified ten genes that,
717 when knocked down in the midgut, significantly affected egg-to-adult emergence, development
718 time, or both traits, in zinc-supplemented media. Perhaps surprisingly, for all but one of our hits,
719 knocking down the gene resulted in greater (rather than lower) resistance to zinc. We speculate
720 that the concentration of zinc chloride we chose to apply in these assays was sufficiently high
721 that it was unlikely for a knockdown genotype to perform significantly worse than the control
722 genotype; A similar effect was noted in a cell-based RNAi screen for zinc toxicity genes, where
723 they suspected the zinc treatment applied was so toxic that it was difficult for worse, RNAi-
724 generated phenotypes to be detected (Mohr et al., 2018).
725
726 Some of the genes identified, such as *GluRIB* and *Nup98-96*, showed effects consistent with a
727 previous cell-based RNAi screen for zinc toxicity (Mohr et al., 2018), providing cross-validation
728 of their role in zinc resistance. We contend that our decision to employ an RNAi knockdown
729 strategy that is specific to the midget (Phillips & Thomas, 2006) makes our conclusion that these
730 genes are involved in zinc resistance more robust than had we used a less tissue specific driver
731 (e.g., a ubiquitous actin- or tubulin-based RNAi knockdown), where unintentional off-target
732 effects could be more likely to bias results. This being said, RNAi knockdowns do not prove that
733 standing variation at the genes we identify drive the initial X-QTL mapping result. Allele
734 replacements via CRISPR/Cas9 would provide more concrete evidence, but are considerably
735 more difficult to achieve.
736
737 The behavior of MTF-1 knockdowns in our RNAi screen was particularly intriguing. Contrary to
738 expectations based on its known role in metal detoxification, in our study knockdown of MTF-1
739 in the midgut led to increased emergence on zinc-supplemented media. This result, combined
740 with previous findings showing increased zinc susceptibility with MTF-1 overexpression
741 (Bahadorani et al., 2010), suggests a more complex relationship between MTF-1 expression
742 levels and zinc resistance than previously thought. Further investigation into the dose-
743 dependent effects of MTF-1 on zinc homeostasis and resistance could yield valuable insights
744 into the regulation of metal detoxification pathways.
745
746 **Founder haplotypes showing the greatest changes in frequency in zinc-selected samples**
747 **tend to be common in the base population:** The observation that founder haplotypes
748 showing substantial changes in frequency due to zinc selection are consistently those at high
749 frequency in the base population is novel. This pattern could reflect the actions of random
750 genetic drift and selection during the creation and maintenance of the DSPR RILs (which we
751 mix to yield our X-QTL base population), or it could indicate that resistance/susceptibility alleles
752 are relatively common in natural populations. In contrast, this observation may have been
753 predictable on theoretical grounds. The change in a founder haplotype frequency in the selected
754 pool versus the base population is proportional to pqs, where p is the frequency of the haplotype
755 in the base population, q is $1 - p$, and s is the strength of selection on the variant (i.e., its effect
756 size). Thus, for a given effect size, we expect more common alleles to show bigger allele
757 frequency shifts, and a corollary is that if the founder allele frequencies in the base population
758 are not each close to $1/F$ (where F is the number of founders) the number of alleles effectively
759 queried is less than F. Further investigation into the frequencies of these alleles in diverse
760 natural populations will be required to provide insights into the evolutionary history and adaptive
761 significance of zinc resistance in *Drosophila*.

762
763 **Conclusion:** Our X-QTL mapping approach, combined with a targeted, tissue-specific RNAi
764 screen, has revealed several genomic regions and specific genes contributing to variation in
765 developmental zinc resistance in *Drosophila*. These findings not only advance our
766 understanding of the genetic architecture of metal toxicity resistance, but also highlight the
767 complex and sometimes counterintuitive nature of metal homeostasis mechanisms. Future
768 studies exploring the molecular mechanisms of these identified genes, their potential roles in
769 resistance to other metals, and their evolutionary significance in natural populations will further
770 elucidate the intricate processes underlying metal toxicity resistance in insects and potentially
771 other organisms.

ACKNOWLEDGEMENTS

This work was supported by NIH awards R01-ES029922 (to SJM) and R01-OD034064 (to SJM and ADL). Computational infrastructure and assistance to authors at KU was provided by the Data Science Core of the Kansas INBRE project (supported by NIH P20-GM103418). The authors acknowledge the Bloomington *Drosophila* Stock Center (P40-OD018537) for supplying strains used in the project.

REFERENCES

Agnew, U. M., & Slesinger, T. L. (2020). Zinc Toxicity. In *StatPearls*. StatPearls Publishing. http://www.ncbi.nlm.nih.gov/books/NBK554548/

Andreini, C., Banci, L., Bertini, I., & Rosato, A. (2006). Counting the Zinc-Proteins Encoded in the Human Genome. *Journal of Proteome Research*, *5*(1), 196–201. https://doi.org/10.1021/pr050361j

Andrews, G. K. (2001). Cellular zinc sensors: MTF-1 regulation of gene expression. *Biometals*, *14*(3), 223–237. https://doi.org/10.1023/A:1012932712483

ATSDR. (2005). *Toxicological profile for Zinc*. Agency for Toxic Substances and Disease Reigstry(ATSDR). https://wwwn.cdc.gov/TSP/ToxProfiles/ToxProfiles.aspx?id=302&tid=54

Bahadorani, S., Mukai, S., Egli, D., & Hilliker, A. J. (2010). Overexpression of metal-responsive transcription factor (MTF-1) in Drosophila melanogaster ameliorates life-span reductions associated with oxidative stress and metal toxicity. *Neurobiology of Aging*, *31*(7), 1215–1226. https://doi.org/10.1016/j.neurobiolaging.2008.08.001

Balamurugan, K., Egli, D., Selvaraj, A., Zhang, B., Georgiev, O., & Schaffner, W. (2004). Metal-responsive transcription factor (MTF-1) and heavy metal stress response in Drosophila and mammalian cells: A functional comparison. *Biological Chemistry*, *385*(7), 597–603. https://doi.org/10.1515/BC.2004.074

Bellen, H. J., Levis, R. W., He, Y., Carlson, J. W., Evans-Holm, M., Bae, E., Kim, J., Metaxakis, A., Savakis, C., Schulze, K. L., Hoskins, R. A., & Spradling, A. C. (2011). The Drosophila gene disruption project: Progress using transposons with distinctive site specificities. *Genetics*, *188*(3), 731–743. https://doi.org/10.1534/genetics.111.126995

Binks, T., Lye, J. C., Camakaris, J., & Burke, R. (2010). Tissue-specific interplay between copper uptake and efflux in Drosophila. *JBIC Journal of Biological Inorganic Chemistry*, *15*(4), 621–628. https://doi.org/10.1007/s00775-010-0629-y

Bridges, C. C., & Zalups, R. K. (2005). Molecular and ionic mimicry and the transport of toxic metals. *Toxicology and Applied Pharmacology*, *204*(3), 274–308. https://doi.org/10.1016/j.taap.2004.09.007

Calap-Quintana, P., González-Fernández, J., Sebastiá-Ortega, N., Llorens, J. V., & Moltó, M. D. (2017). Drosophila melanogaster Models of Metal-Related Human Diseases and Metal Toxicity. *International Journal of Molecular Sciences*, *18*(7), Article 7. https://doi.org/10.3390/ijms18071456

Chandler, C. H., Chari, S., & Dworkin, I. (2013). Does your gene need a background check? How genetic background impacts the analysis of mutations, genes, and evolution. *Trends in Genetics : TIG*, *29*(6), Article 6. https://doi.org/10.1016/j.tig.2013.01.009

Collaborative Cross Consortium. (2012). The genome architecture of the Collaborative Cross mouse genetic reference population. *Genetics*, *190*(2), 389–401. https://doi.org/10.1534/genetics.111.132639

Cooper, R. G. (2008). Zinc toxicology following particulate inhalation. *Indian Journal of Occupational and Environmental Medicine*, *12*(1), Article 1. https://doi.org/10.4103/0019-5278.40809

Earley, B. J., Cubillas, C., Warnhoff, K., Ahmad, R., Alcantar, A., Lyon, M. D., Schneider, D. L., & Kornfeld, K. (2021). Cadmium hijacks the high zinc response by binding and activating the HIZR-1

818 nuclear receptor. *Proceedings of the National Academy of Sciences*, *118*(42), e2022649118.
819 https://doi.org/10.1073/pnas.2022649118

820 Egli, D., Selvaraj, A., Yepiskoposyan, H., Zhang, B., Hafen, E., Georgiev, O., & Schaffner, W. (2003).
821 Knockout of 'metal-responsive transcription factor' MTF-1 in Drosophila by homologous recombination
822 reveals its central role in heavy metal homeostasis. *The EMBO Journal*, *22*(1), 100–108.
823 https://doi.org/10.1093/emboj/cdg012

824 Ehrenreich, I. M., Torabi, N., Jia, Y., Kent, J., Martis, S., Shapiro, J. A., Gresham, D., Caudy, A. A., &
825 Kruglyak, L. (2010). Dissection of genetically complex traits with extremely large pools of yeast
826 segregants. *Nature*, *464*(7291), Article 7291. https://doi.org/10.1038/nature08923

827 Evans, K. S., Brady, S. C., Bloom, J. S., Tanny, R. E., Cook, D. E., Giuliani, S. E., Hippleheuser, S. W.,
828 Zamanian, M., & Andersen, E. C. (2018). Shared Genomic Regions Underlie Natural Variation in
829 Diverse Toxin Responses. *Genetics*, *210*(4), 1509–1525. https://doi.org/10.1534/genetics.118.301311

830 Evans, K. S., Zdraljevic, S., Stevens, L., Collins, K., Tanny, R. E., & Andersen, E. C. (2020). Natural
831 variation in the sequestosome-related gene, sqst-5, underlies zinc homeostasis in Caenorhabditis elegans.
832 *PLOS Genetics*, *16*(11), e1008986. https://doi.org/10.1371/journal.pgen.1008986

833 Everman, E. R., Cloud-Richardson, K. M., & Macdonald, S. J. (2021). Characterizing the genetic basis of
834 copper toxicity in Drosophila reveals a complex pattern of allelic, regulatory, and behavioral variation.
835 *Genetics*, *217*(1), 1–20. https://doi.org/10.1093/genetics/iyaa020

836 Feingold, D., Starc, T., O'Donnell, M. J., Nilson, L., & Dent, J. A. (2016). The orphan pentameric ligand-
837 gated ion channel pHCl-2 is gated by pH and regulates fluid secretion in Drosophila Malpighian tubules.
838 *Journal of Experimental Biology*, *219*(17), 2629–2638. https://doi.org/10.1242/jeb.141069

839 Fischer Walker, C. L., Ezzati, M., & Black, R. E. (2009). Global and regional child mortality and burden
840 of disease attributable to zinc deficiency. *European Journal of Clinical Nutrition*, *63*(5), Article 5.
841 https://doi.org/10.1038/ejcn.2008.9

842 Fu, Z., & Xi, S. (2020). The effects of heavy metals on human metabolism. *Toxicology Mechanisms and*
843 *Methods*, *30*(3), 167–176. https://doi.org/10.1080/15376516.2019.1701594

844 Fukada, T., Yamasaki, S., Nishida, K., Murakami, M., & Hirano, T. (2011). Zinc homeostasis and
845 signaling in health and diseases: Zinc Signaling. *Journal of Biological Inorganic Chemistry*, *16*(7),
846 Article 7. https://doi.org/10.1007/s00775-011-0797-4

847 Gaither, L. A., & Eide, D. J. (2001). The human ZIP1 transporter mediates zinc uptake in human K562
848 erythroleukemia cells. *The Journal of Biological Chemistry*, *276*(25), Article 25.
849 https://doi.org/10.1074/jbc.M101772200

850 Goutam Mukherjee, A., Ramesh Wanjari, U., Renu, K., Vellingiri, B., & Valsala Gopalakrishnan, A.
851 (2022). Heavy metal and metalloid—Induced reproductive toxicity. *Environmental Toxicology and*
852 *Pharmacology*, *92*, 103859. https://doi.org/10.1016/j.etap.2022.103859

853 Gramates, L. S., Agapite, J., Attrill, H., Calvi, B. R., Crosby, M. A., dos Santos, G., Goodman, J. L.,
854 Goutte-Gattat, D., Jenkins, V. K., Kaufman, T., Larkin, A., Matthews, B. B., Millburn, G., Strelets, V. B.,
855 & the FlyBase Consortium. (2022). FlyBase: A guided tour of highlighted features. *Genetics*, *220*(4),
856 iyac035. https://doi.org/10.1093/genetics/iyac035

Guo, L., Lichten, L. A., Ryu, M.-S., Liuzzi, J. P., Wang, F., & Cousins, R. J. (2010). STAT5-glucocorticoid receptor interaction and MTF-1 regulate the expression of ZnT2 (Slc30a2) in pancreatic acinar cells. *Proceedings of the National Academy of Sciences of the United States of America*, *107*(7), 2818–2823. https://doi.org/10.1073/pnas.0914941107

Harold, S. (2014). Chapter 61 Zinc. In Gunnar F. Nordeberg, Bruce A. Fowler, & Monica Nordberg (Eds.), *Handbook on the Toxicology of Metals* (4th ed., Vol. 1, pp. 1369–1385). Elsevier Science & Technology. http://ebookcentral.proquest.com/lib/ku/detail.action?docID=1757714

Hoffman, H. N., Phyliky, R. L., & Fleming, C. R. (1988). Zinc-induced copper deficiency. *Gastroenterology*, *94*(2), 508–512. https://doi.org/10.1016/0016-5085(88)90445-3

Irving, J. A., Mattman, A., Lockitch, G., Farrell, K., & Wadsworth, L. D. (2003). Element of caution: A case of reversible cytopenias associated with excessive zinc supplementation. *CMAJ: Canadian Medical Association Journal*, *169*(2), 129–131.

Jaishankar, M., Tseten, T., Anbalagan, N., Mathew, B. B., & Beeregowda, K. N. (2014). Toxicity, mechanism and health effects of some heavy metals. *Interdisciplinary Toxicology*, *7*(2), Article 2. https://doi.org/10.2478/intox-2014-0009

Kambe, T., Tsuji, T., Hashimoto, A., & Itsumura, N. (2015). The Physiological, Biochemical, and Molecular Roles of Zinc Transporters in Zinc Homeostasis and Metabolism. *Physiological Reviews*, *95*(3), Article 3. https://doi.org/10.1152/physrev.00035.2014

Karri, V., Schuhmacher, M., & Kumar, V. (2016). Heavy metals (Pb, Cd, As and MeHg) as risk factors for cognitive dysfunction: A general review of metal mixture mechanism in brain. *Environmental Toxicology and Pharmacology*, *48*, 203–213. https://doi.org/10.1016/j.etap.2016.09.016

Kim, J.-J., Kim, Y.-S., & Kumar, V. (2019). Heavy metal toxicity: An update of chelating therapeutic strategies. *Journal of Trace Elements in Medicine and Biology: Organ of the Society for Minerals and Trace Elements (GMS)*, *54*, 226–231. https://doi.org/10.1016/j.jtemb.2019.05.003

King, E. G., Macdonald, S. J., & Long, A. D. (2012). Properties and Power of the Drosophila Synthetic Population Resource for the Routine Dissection of Complex Traits. *Genetics*, *191*(3), 935–949. https://doi.org/10.1534/genetics.112.138537

King, E. G., Merkes, C. M., McNeil, C. L., Hoofer, S. R., Sen, S., Broman, K. W., Long, A. D., & Macdonald, S. J. (2012). Genetic dissection of a model complex trait using the Drosophila Synthetic Population Resource. *Genome Research*, *22*(8), 1558–1566. https://doi.org/10.1101/gr.134031.111

Knowles DA, Burrows CK, Blischak JD, Patterson KM, Serie DJ, Norton N, Ober C, Pritchard JK, Gilad Y. Determining the genetic basis of anthracycline-cardiotoxicity by molecular response QTL mapping in induced cardiomyocytes. Elife. 2018 May 8;7:e33480. doi: 10.7554/eLife.33480. PMID: 29737278; PMCID: PMC6010343.

Langmade, S. J., Ravindra, R., Daniels, P. J., & Andrews, G. K. (2000). The transcription factor MTF-1 mediates metal regulation of the mouse ZnT1 gene. *The Journal of Biological Chemistry*, *275*(44), 34803–34809. https://doi.org/10.1074/jbc.M007339200

Lasater, M. (2017). Zinc Toxicity Because of Denture Adhesive. *Journal of Neuroscience Nursing*, *49*(1), 23. https://doi.org/10.1097/JNN.0000000000000203

Lemaitre, B., & Miguel-Aliaga, I. (2013). The Digestive Tract of Drosophila melanogaster. *Annual Review of Genetics*, *47*(1), 377–404. https://doi.org/10.1146/annurev-genet-111212-133343

Lemire, J., Mailloux, R., & Appanna, V. D. (2008). Zinc toxicity alters mitochondrial metabolism and leads to decreased ATP production in hepatocytes. *Journal of Applied Toxicology: JAT*, *28*(2), Article 2. https://doi.org/10.1002/jat.1263

Li, H. (2011). A statistical framework for SNP calling, mutation discovery, association mapping and population genetical parameter estimation from sequencing data. *Bioinformatics*, *27*(21), 2987–2993. https://doi.org/10.1093/bioinformatics/btr509

Li, H. (2013). *Aligning sequence reads, clone sequences and assembly contigs with BWA-MEM* (arXiv:1303.3997). arXiv. https://doi.org/10.48550/arXiv.1303.3997

Lichten, L. A., Ryu, M.-S., Guo, L., Embury, J., & Cousins, R. J. (2011). MTF-1-Mediated Repression of the Zinc Transporter Zip10 Is Alleviated by Zinc Restriction. *PLOS ONE*, *6*(6), e21526. https://doi.org/10.1371/journal.pone.0021526

Linder, R. A., Majumder, A., Chakraborty, M., & Long, A. (2020). Two Synthetic 18-Way Outcrossed Populations of Diploid Budding Yeast with Utility for Complex Trait Dissection. *Genetics*, *215*(2), 323–342. https://doi.org/10.1534/genetics.120.303202

Luo, M., Finet, C., Cong, H., Wei, H., & Chung, H. (2020). The evolution of insect metallothioneins. *Proceedings of the Royal Society B: Biological Sciences*, *287*(1937), 20202189. https://doi.org/10.1098/rspb.2020.2189

Lye, J. C., Richards, C. D., Dechen, K., Paterson, D., Jonge, M. D. de, Howard, D. L., Warr, C. G., & Burke, R. (2012). Systematic functional characterization of putative zinc transport genes and identification of zinc toxicosis phenotypes in Drosophila melanogaster. *Journal of Experimental Biology*, *215*(18), Article 18. https://doi.org/10.1242/jeb.069260

Macdonald, S. J., Cloud-Richardson, K. M., Sims-West, D. J., & Long, A. D. (2022). Powerful, efficient QTL mapping in Drosophila melanogaster using bulked phenotyping and pooled sequencing. *Genetics*, *220*(3), iyab238. https://doi.org/10.1093/genetics/iyab238

Macdonald, S. J., & Long, A. D. (2022). Discovery of malathion resistance QTL in Drosophila melanogaster using a bulked phenotyping approach. *G3 Genes|Genomes|Genetics*, jkac279. https://doi.org/10.1093/g3journal/jkac279

Maret, W. (2008). Metallothionein redox biology in the cytoprotective and cytotoxic functions of zinc. *Experimental Gerontology*, *43*(5), 363–369. https://doi.org/10.1016/j.exger.2007.11.005

Maret, W. (2013). Zinc Biochemistry: From a Single Zinc Enzyme to a Key Element of Life12. *Advances in Nutrition*, *4*(1), Article 1. https://doi.org/10.3945/an.112.003038

Michelmore, R. W., Paran, I., & Kesseli, R. V. (1991). Identification of markers linked to disease-resistance genes by bulked segregant analysis: A rapid method to detect markers in specific genomic regions by using segregating populations. *Proceedings of the National Academy of Sciences of the United States of America*, *88*(21), 9828–9832. https://doi.org/10.1073/pnas.88.21.9828

Mohr, S. E., Rudd, K., Hu, Y., Song, W. R., Gilly, Q., Buckner, M., Housden, B. E., Kelley, C., Zirin, J., Tao, R., Amador, G., Sierzputowska, K., Comjean, A., & Perrimon, N. (2018). Zinc Detoxification: A

Functional Genomics and Transcriptomics Analysis in Drosophila melanogaster Cultured Cells. *G3: Genes, Genomes, Genetics*, *8*(2), Article 2. https://doi.org/10.1534/g3.117.300447

Moyson, S., Vissenberg, K., Fransen, E., Blust, R., & Husson, S. J. (2018). Mixture effects of copper, cadmium, and zinc on mortality and behavior of Caenorhabditis elegans. *Environmental Toxicology and Chemistry*, *37*(1), 145–159. https://doi.org/10.1002/etc.3937

Navarro, J. A., & Schneuwly, S. (2017). Copper and Zinc Homeostasis: Lessons from Drosophila melanogaster. *Frontiers in Genetics*, *8*. https://doi.org/10.3389/fgene.2017.00223

Noel, N. E., & Ruthman, J. C. (1988). Elevated serum zinc levels in metal fume fever. *The American Journal of Emergency Medicine*, *6*(6), 609–610. https://doi.org/10.1016/0735-6757(88)90103-9

Palmiter, R. D., & Findley, S. D. (1995). Cloning and functional characterization of a mammalian zinc transporter that confers resistance to zinc. *The EMBO Journal*, *14*(4), Article 4.

Perkins, L. A., Holderbaum, L., Tao, R., Hu, Y., Sopko, R., McCall, K., Yang-Zhou, D., Flockhart, I., Binari, R., Shim, H.-S., Miller, A., Housden, A., Foos, M., Randkelv, S., Kelley, C., Namgyal, P., Villalta, C., Liu, L.-P., Jiang, X., … Perrimon, N. (2015). The Transgenic RNAi Project at Harvard Medical School: Resources and Validation. *Genetics*, *201*(3), 843–852. https://doi.org/10.1534/genetics.115.180208

Phillips, M. D., & Thomas, G. H. (2006). Brush border spectrin is required for early endosome recycling in Drosophila. *Journal of Cell Science*, *119*(7), 1361–1370. https://doi.org/10.1242/jcs.02839

Power, R. S., & de Pomerai, D. I. (1999). Effect of Single and Paired Metal Inputs in Soil on a Stress-Inducible Transgenic Nematode. *Archives of Environmental Contamination and Toxicology*, *37*(4), 503–511. https://doi.org/10.1007/s002449900545

Prasad, A. S. (2013). Discovery of Human Zinc Deficiency: Its Impact on Human Health and Disease. *Advances in Nutrition*, *4*(2), 176–190. https://doi.org/10.3945/an.112.003210

Redhai, S., Pilgrim, C., Gaspar, P., Giesen, L. van, Lopes, T., Riabinina, O., Grenier, T., Milona, A., Chanana, B., Swadling, J. B., Wang, Y.-F., Dahalan, F., Yuan, M., Wilsch-Brauninger, M., Lin, W., Dennison, N., Capriotti, P., Lawniczak, M. K. N., Baines, R. A., … Miguel-Aliaga, I. (2020). An intestinal zinc sensor regulates food intake and developmental growth. *Nature*, *580*(7802), 263–268. https://doi.org/10.1038/s41586-020-2111-5

Rehman, K., Fatima, F., Waheed, I., & Akash, M. S. H. (2018). Prevalence of exposure of heavy metals and their impact on health consequences. *Journal of Cellular Biochemistry*, *119*(1), Article 1. https://doi.org/10.1002/jcb.26234

Remnant, E. J., Williams, A., Lumb, C., Yang, Y. T., Chan, J., Duchêne, S., Daborn, P. J., Batterham, P., & Perry, T. (2016). Evolution, Expression, and Function of Nonneuronal Ligand-Gated Chloride Channels in Drosophila melanogaster. *G3 Genes|Genomes|Genetics*, *6*(7), 2003–2012. https://doi.org/10.1534/g3.116.029546

Romero, M. F., Henry, D., Nelson, S., Harte, P. J., Dillon, A. K., & Sciortino, C. M. (2000). Cloning and Characterization of a Na+-driven Anion Exchanger (NDAE1): A NEW BICARBONATE TRANSPORTER*. *Journal of Biological Chemistry*, *275*(32), 24552–24559. https://doi.org/10.1074/jbc.M003476200

Sciortino, C. M., Shrode, L. D., Fletcher, B. R., Harte, P. J., & Romero, M. F. (2001). Localization of endogenous and recombinant Na+-driven anion exchanger protein NDAE1 fromDrosophila melanogaster. *American Journal of Physiology-Cell Physiology*, *281*(2), C449–C463. https://doi.org/10.1152/ajpcell.2001.281.2.C449

Sensi, S. L., Paoletti, P., Bush, A. I., & Sekler, I. (2009). Zinc in the physiology and pathology of the CNS. *Nature Reviews Neuroscience*, *10*(11), Article 11. https://doi.org/10.1038/nrn2734

Sittig, L. J., Carbonetto, P., Engel, K. A., Krauss, K. S., Barrios-Camacho, C. M., & Palmer, A. A. (2016). Genetic Background Limits Generalizability of Genotype-Phenotype Relationships. *Neuron*, *91*(6), Article 6. https://doi.org/10.1016/j.neuron.2016.08.013

Soetaert, K., Van den Meersche, K., & van Oevelen, D. (2009). *LimSolve, Solving Linear Inverse Models* (Version 1.5.1) [R].

Stuart, G. W., Searle, P. F., & Palmiter, R. D. (1985). Identification of multiple metal regulatory elements in mouse metallothionein-I promoter by assaying synthetic sequences. *Nature*, *317*(6040), Article 6040. https://doi.org/10.1038/317828a0

Tchounwou, P. B., Yedjou, C. G., Patlolla, A. K., & Sutton, D. J. (2012). Heavy Metals Toxicity and the Environment. *EXS*, *101*, 133–164. https://doi.org/10.1007/978-3-7643-8340-4_6

Tennessen, J. M., Baker, K. D., Lam, G., Evans, J., & Thummel, C. S. (2011). The Drosophila Estrogen-Related Receptor Directs a Metabolic Switch that Supports Developmental Growth. *Cell Metabolism*, *13*(2), 139–148. https://doi.org/10.1016/j.cmet.2011.01.005

Wang X, Kruglyak L. Genetic basis of haloperidol resistance in Saccharomyces cerevisiae is complex and dose dependent. PLoS Genet. 2014 Dec 18;10(12):e1004894. doi: 10.1371/journal.pgen.1004894. PMID: 25521586; PMCID: PMC4270474.

Wang, Y., Wimmer, U., Lichtlen, P., Inderbitzin, D., Stieger, B., Meier, P. J., Hunziker, L., Stallmach, T., Forrer, R., Rülicke, T., Georgiev, O., & Schaffner, W. (2004). Metal-responsive transcription factor-1 (MTF-1) is essential for embryonic liver development and heavy metal detoxification in the adult liver. *The FASEB Journal*, *18*(10), 1071–1079. https://doi.org/10.1096/fj.03-1282com

Warrington, N. M., Zhu, G., Dy, V., Heath, A. C., Madden, P. A. F., Hemani, G., Kemp, J. P., Mcmahon, G., St Pourcain, B., Timpson, N. J., Taylor, C. M., Golding, J., Lawlor, D. A., Steer, C., Montgomery, G. W., Martin, N. G., Davey Smith, G., Evans, D. M., & Whitfield, J. B. (2015). Genome-wide association study of blood lead shows multiple associations near ALAD. *Human Molecular Genetics*, *24*(13), 3871–3879. https://doi.org/10.1093/hmg/ddv112

Widmayer SJ, Crombie TA, Nyaanga JN, Evans KS, Andersen EC. C. elegans toxicant responses vary among genetically diverse individuals. Toxicology. 2022 Sep;479:153292. doi: 10.1016/j.tox.2022.153292. Epub 2022 Aug 20. PMID: 35995124; PMCID: PMC9573778.

Willems, G., Dräger, D. B., Courbot, M., Godé, C., Verbruggen, N., & Saumitou-Laprade, P. (2007). The Genetic Basis of Zinc Tolerance in the Metallophyte Arabidopsis halleri ssp. halleri (Brassicaceae): An Analysis of Quantitative Trait Loci. *Genetics*, *176*(1), 659–674. https://doi.org/10.1534/genetics.106.064485

Willis, M. S., Monaghan, S. A., Miller, M. L., McKenna, R. W., Perkins, W. D., Levinson, B. S., Bhushan, V., & Kroft, S. H. (2005). Zinc-induced copper deficiency: A report of three cases initially

1014 recognized on bone marrow examination. *American Journal of Clinical Pathology*, *123*(1), 125–131.
1015 https://doi.org/10.1309/v6gvyw2qtyd5c5pj

1016 Xenakis, J. G., Douillet, C., Bell, T. A., Hock, P., Farrington, J., Liu, T., Murphy, C. E. Y., Saraswatula,
1017 A., Shaw, G. D., Nativio, G., Shi, Q., Venkatratnam, A., Zou, F., Fry, R. C., Stýblo, M., & Pardo-Manuel
1018 de Villena, F. (2022). An interaction of inorganic arsenic exposure with body weight and composition on
1019 type 2 diabetes indicators in Diversity Outbred mice. *Mammalian Genome: Official Journal of the*
1020 *International Mammalian Genome Society*, *33*(4), 575–589. https://doi.org/10.1007/s00335-022-09957-w

1021 Xiao, G., & Zhou, B. (2016). What can flies tell us about zinc homeostasis? *Archives of Biochemistry and*
1022 *Biophysics*, *611*, 134–141. https://doi.org/10.1016/j.abb.2016.04.016

1023 Yepiskoposyan, H., Egli, D., Fergestad, T., Selvaraj, A., Treiber, C., Multhaup, G., Georgiev, O., &
1024 Schaffner, W. (2006). Transcriptome response to heavy metal stress in Drosophila reveals a new zinc
1025 transporter that confers resistance to zinc. *Nucleic Acids Research*, *34*(17), 4866–4877.
1026 https://doi.org/10.1093/nar/gkl606

1027 Yiwen, W., Xiaohan, T., Chunfeng, Z., Xiaoyu, Y., Yaodong, M., & Huanhuan, Q. (2022). Genetics of
1028 metallothioneins in Drosophila melanogaster. *Chemosphere*, *288*, 132562.
1029 https://doi.org/10.1016/j.chemosphere.2021.132562

1030 Zhang, B., Egli, D., Georgiev, O., & Schaffner, W. (2001). The Drosophila Homolog of Mammalian Zinc
1031 Finger Factor MTF-1 Activates Transcription in Response to Heavy Metals. *Molecular and Cellular*
1032 *Biology*, *21*(14), 4505–4514. https://doi.org/10.1128/MCB.21.14.4505-4514.2001

1033 Zhang, J., Chen, K., Pang, Y., Naveed, S. A., Zhao, X., Wang, X., Wang, Y., Dingkuhn, M., Pasuquin, J.,
1034 Li, Z., & Xu, J. (2017). QTL mapping and candidate gene analysis of ferrous iron and zinc toxicity
1035 tolerance at seedling stage in rice by genome-wide association study. *BMC Genomics*, *18*.
1036 https://doi.org/10.1186/s12864-017-4221-5

1037 Zheng, D., Feeney, G. P., Kille, P., & Hogstrand, C. (2008). Regulation of ZIP and ZnT zinc transporters
1038 in zebrafish gill: Zinc repression of ZIP10 transcription by an intronic MRE cluster. *Physiological*
1039 *Genomics*, *34*(2), 205–214. https://doi.org/10.1152/physiolgenomics.90206.2008

1040 Zhou, S., Luoma, S. E., St. Armour, G. E., Thakkar, E., Mackay, T. F. C., & Anholt, R. R. H. (2017). A
1041 Drosophila model for toxicogenomics: Genetic variation in susceptibility to heavy metal exposure. *PLoS*
1042 *Genetics*, *13*(7), e1006907. https://doi.org/10.1371/journal.pgen.1006907

1043

1044 TABLES

1045

1046 **Table 1. Mapped zinc resistance QTL.**

1047

QTL	Chromosome	Peak Position (bp) [a]	Physical Interval (bp) [a]	QTL Size (Kb)	QTL Size (cM)	Genes [b]	Candidate Genes
A	X	13,945,053	13,796,451 – 14,093,253	300	1.30	21	*ben*
B	2L	7,135,043	6,829,342 – 7,325,061	560	2.20	58	*Gart* [c], *Mnn1*, *CG4496*, *Ndae1*
C	2R	15,413,541	15,116,465 – 15,886,141	780	2.85	88	*Trpm*, *Vha36-1* [c], *Vha14-1* [c]
D	3L	8,925,893	8,352,067 – 9,512,583	1160	4.70	166	*GluRIB*, *Hsp22*, *MTF-1*
E	3R	18,864,745	18,717,419 – 18,987,824	280	0.65	30	*CG14302* [c], *Mekk1*, *Octα2R*, *Xrp1*, *ATPsynD* [d]
F	3R	23,906,956	23,458,263 – 24,716,284	1250	4.50	190	*RanBP3*, *Nup98-96*, *Ndc1*
G	3R	30,848,984	30,368,845 – 31,020,051	820	0.80	78	*Fer1HCH*, *Fer2LCH*, *dj-1β*, *pHCl-2* [d], *CG11318* [d]

1048

1049 [a] Physical positions are determined from the corresponding genetic positions, and are based on Release 6 of the *D. melanogaster* reference
1050 genome. Intervals are defined as 3 $-\log_{10}(P)$ drops from the QTL peak LOD score position.

1051

1052 [b] The number of annotated protein-coding genes. Annotations sourced from Flybase release FB2022_06 (Gramates et al., 2022).

1053

1054 [c] These genes did not have TRiP UAS-RNAi strains available from the BDSC so were not tested via RNAi.

1055

1056 [d] Genes not within the final set of X-QTL intervals. When genes were selected for functional testing a slightly different analysis scheme was
1057 being employed to that reported here. *ATPsynD* is within 120-kb of the left end of the QTL-E interval, and *CG11318* and *pHCl-2* are within 90-
1058 kb and 290-kb of the left end of the QTL-G interval, respectively. We note that QTL-G is at the terminal end of chromosome 3R (Figure 1).

1059

1060

1061 **Table 2. Effects of RNAi knockdown on emergence and development time.**
1062

QTL	Gene	UAS ID	Emergence [a]						Development Time [b]					
			Change in Emergence	attP2 (–0.429)	attP40 (–0.178)	GFP (–0.375)	Luc (–0.147)	Hit	Developmental Delay	attP2 (1.57)	attP40 (2.16)	GFP (1.50)	Luc (1.43)	Hit
A	*ben*	28721	–0.294	***	*	ns	***		2.037	ns	ns	ns	ns	
B	*CG4496*	51428	–0.197	***	ns	**	ns		1.742	ns	*	ns	*	
B	*Mnn1*	51862	–0.161	***	ns	***	ns		1.266	ns	ns	ns	ns	
B	*Ndae1*	62177	–0.151	***	ns	***	ns		2.367	**	*	***	***	X
C	*Trpm*	51713	–0.073	***	*	***	ns		1.686	ns	*	ns	ns	
C	*Trpm*	57871	–0.089	***	*	***	ns		1.324	ns	***	ns	ns	
D	*GluRIB*	67843	–0.199	***	ns	**	ns		0.696	***	***	***	***	X
D	*Hsp22*	41709	–0.125	***	ns	***	ns		0.872	***	***	***	***	X
D	*MTF-1*	33381	–0.047	***	*	***	*	X	1.831	ns	*	*	ns	
D	*MTF-1*	34094	–0.126	***	ns	***	ns		1.674	ns	ns	*	*	
E	*ATPsynD*	33740	–0.192	***	ns	**	ns		0.545	**	***	***	***	X
E	*Mekk1*	28587	–0.274	***	*	ns	**		1.234	ns	***	*	*	
E	*Octa2R*	50678	–0.142	***	ns	***	ns		1.334	*	***	*	*	X
E	*Xrp1*	34521	–0.061	***	*	***	*	X	1.737	ns	*	ns	ns	
E	*Xrp1*	51054	–0.074	***	*	***	ns		0.611	***	***	***	***	X
F	*Ndc1*	67275	–0.073	***	*	***	ns		1.548	ns	***	ns	ns	
F	*Nup98-96*	28562	–0.240	***	ns	*	*		0.896	**	***	***	***	X
F	*RanBP3*	40948	–0.117	***	ns	***	ns		1.624	ns	*	ns	ns	
G	*CG11318*	51792	–0.080	***	*	***	ns		1.413	ns	***	ns	ns	
G	*dj-1β*	38999	–0.188	***	ns	**	ns		0.415	**	***	***	***	X
G	*pHCl-2*	26003	–0.055	***	*	***	*	X	0.838	**	***	***	***	X

1063
1064 The phenotypes presented are derived from *mex1*-GAL4:UAS-RNAi strains and their controls. Each RNAi genotype was compared to each control separately,
1065 and the effect of the genotype-by-treatment interaction was evaluated: ns, not significant; *, $p < 0.05$; **, $p < 0.0024$; ***, $p < 0.0003$. An RNAi is considered
1066 a "hit" when all tests are significant at $p < 0.05$, and at least one is significant at $p < 0.0003$. See Supplementary Table 6 for full ANOVA details.
1067
1068 [a] The change in emergence for each RNAi genotype is the emergence in zinc treatment minus the emergence in the water control treatment. These values
1069 are routinely negative; zinc treatment reduces emergence. The equivalent values for each control genotype (attP2, attP40, GFP, Luc) are provided in the
1070 column headers for comparison.
1071 [b] Developmental delay for each RNAi genotype is the development time in the zinc treatment minus that in the water control treatment. The values are
1072 routinely positive; development is longer (i.e., is delayed) in zinc media. The equivalent values for each control genotype (attP2, attP40, GFP, Luc) are
1073 provided in the column headers for comparison.

1074 FIGURES
1075
1076
1077
1078
1079

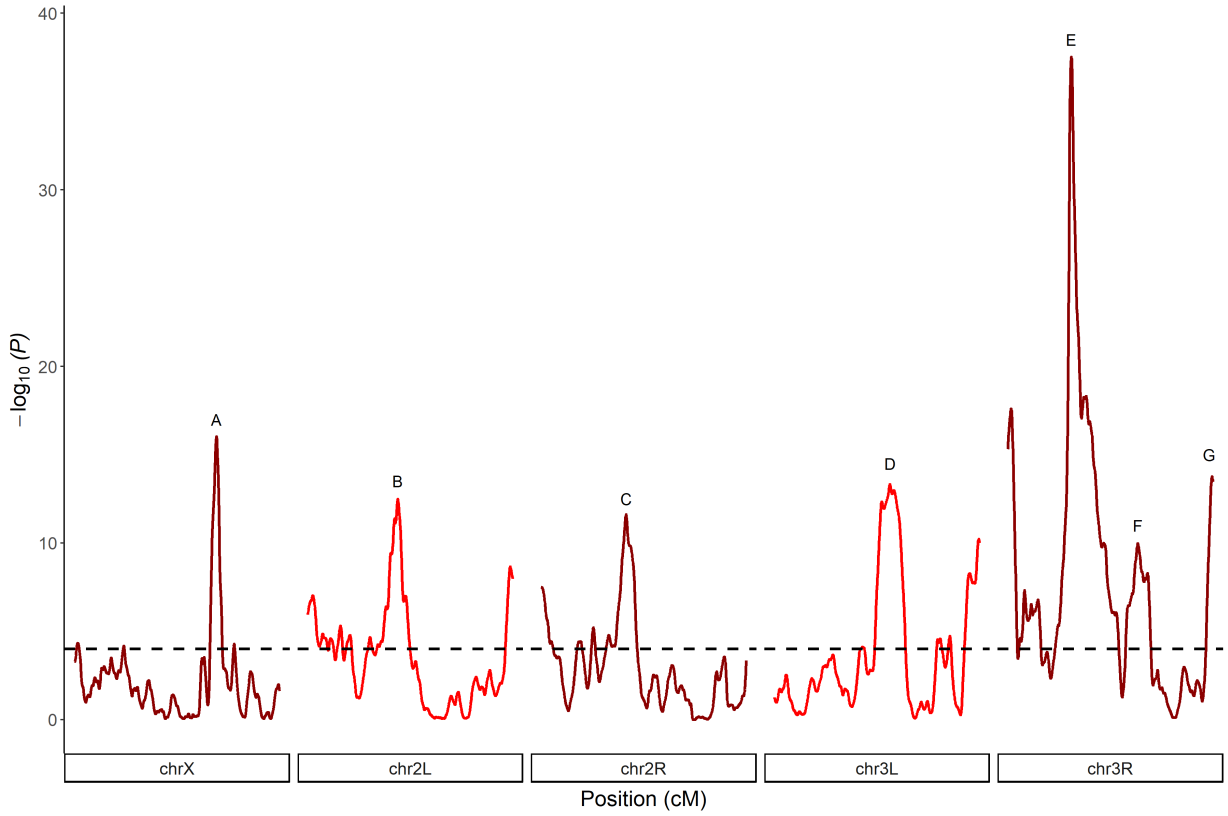

1080
1081
1082 **Figure 1: Locations of 7 mapped zinc-resistance loci.** Using X-QTL mapping we identified 7
1083 QTL – A through G – for zinc resistance throughout the genome. QTL have peaks greater than
1084 a genomewide significance threshold of $-\log_{10}(P)=4$ (horizontal dashed line). Additional peaks
1085 above this threshold are also apparent, but these are primarily located in centromeric regions,
1086 and while they may represent true susceptibility loci they implicate very large physical regions,
1087 and further dissection is challenging.

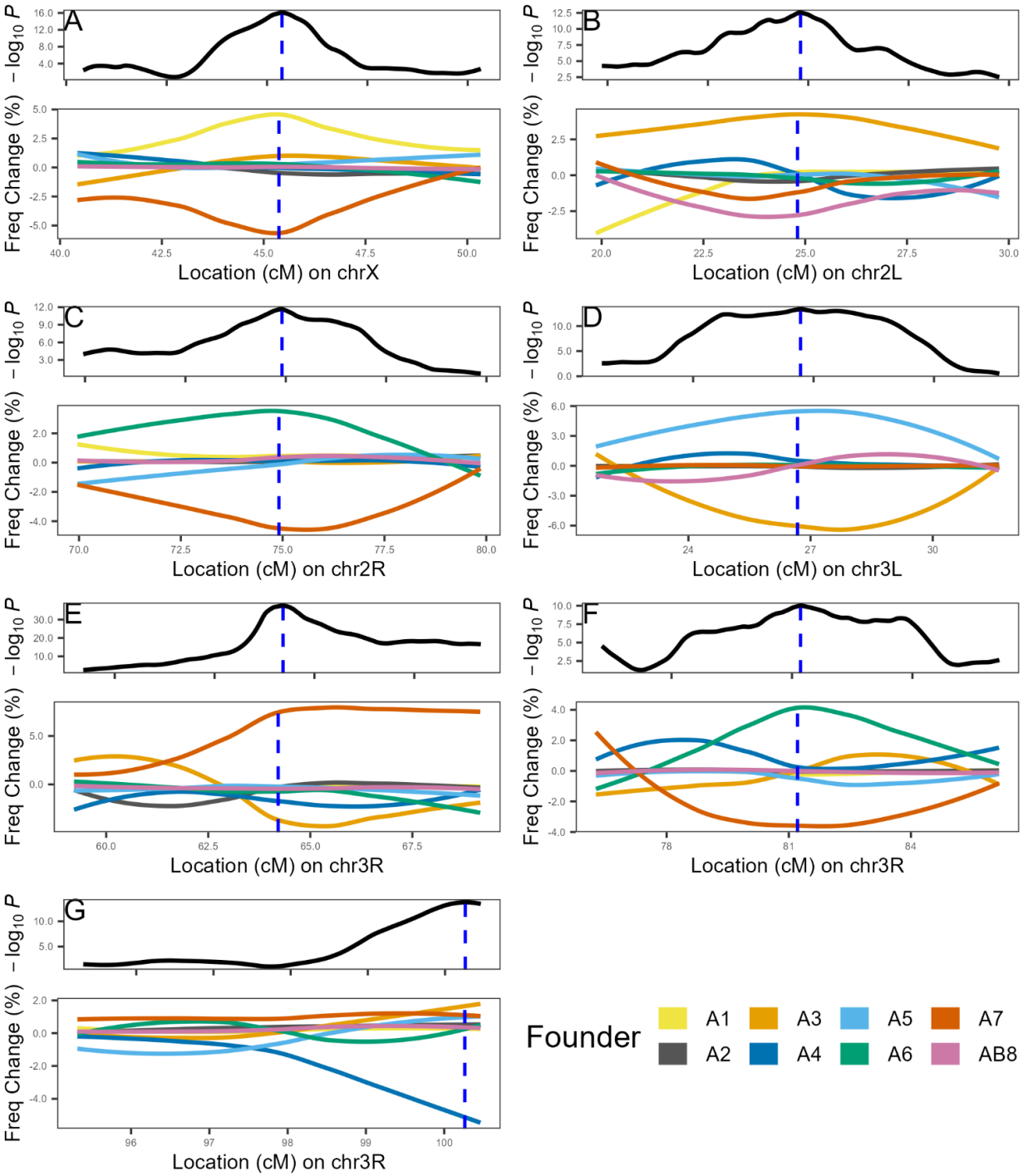

Figure 2: Change in founder haplotype frequencies at mapped QTL. For each of the 7 QTL (A-G) we show – top panels – a zoomed-in view of each QTL region from Figure 1, with a blue vertical dashed line highlighting the peak of the QTL. The bottom panels plot the change in the frequency of each founder haplotype between treatments (zinc-selected minus control); A frequency change above zero implies the founder is more frequent in the zinc-selected population. QTL-G is at the end of chromosome 3R, which is why the peak is on the right-hand side of the plot. (See also Supplementary Figure 2).

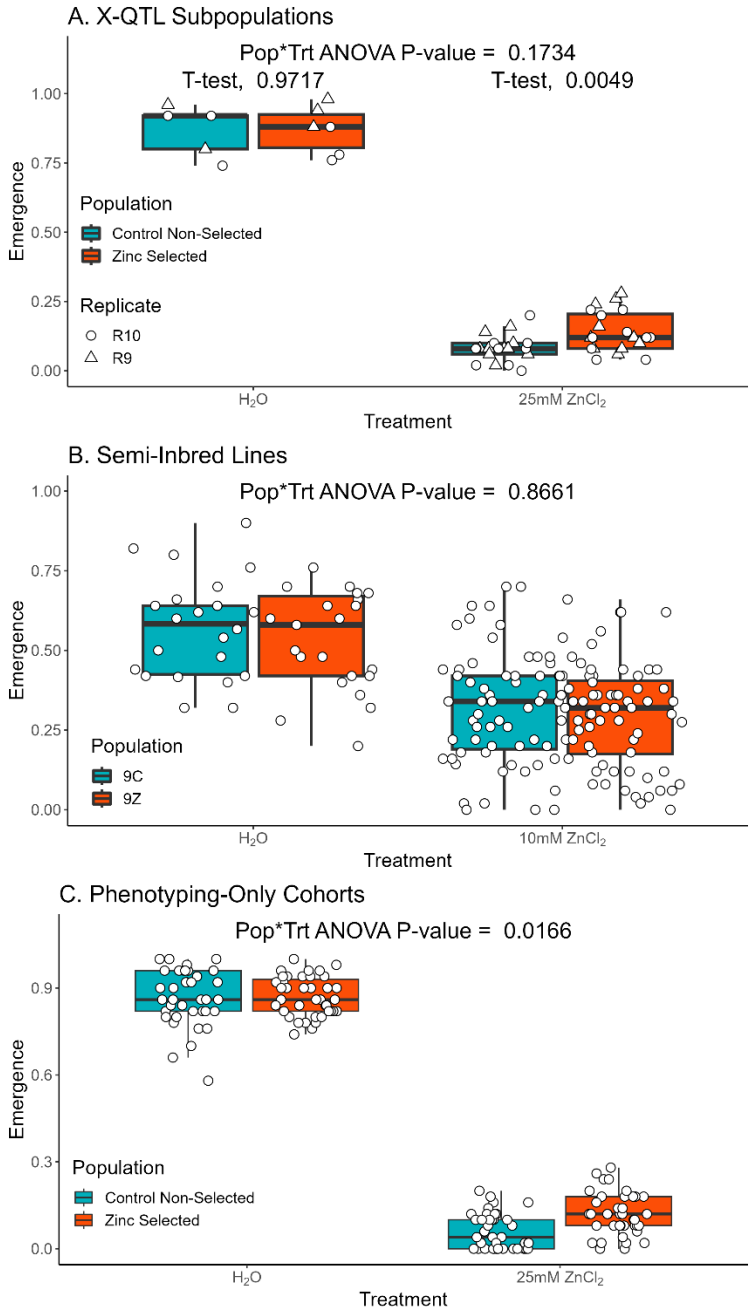

Figure 3: Zinc-selected populations show increased egg-to-adult emergence on zinc-containing media. We raised embryos from several different populations in both control media, and media containing a high zinc chloride concentration. Each point in the figure is the fraction of adults that emerged from a given test vial. (A) Outbred animals derived from X-QTL replicate 9 and 10 (R9, R10) samples; There is no significant population-by-treatment interaction, but zinc-selected populations show higher emergence on zinc media (*t*-test, $p < 0.005$). (B) Semi-inbred lines derived from the R9 and R10 Control and Zinc-selected cohorts; no significant population-by-treatment interaction. (C) Outbred animals generated in an analogous fashion to our X-QTL design; we see a significant population-by-treatment interaction ($p < 0.02$) with zinc-selected animals showing greater emergence on zinc-containing treatment. See Supplementary Table 3 for full details of the ANOVA statistical analyses.

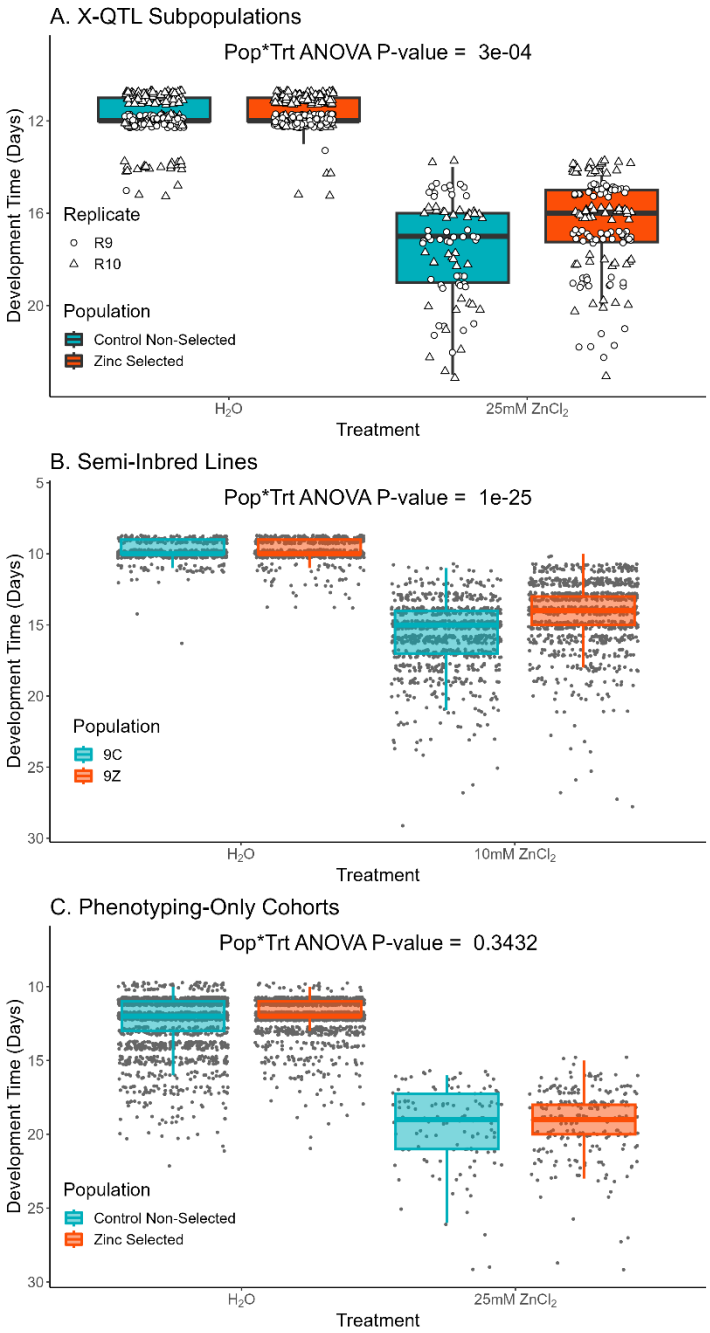

Figure 4: Zinc-selected populations show relatively faster development on zinc-containing media. We raised embryos from several different populations in both control media, and media containing a high zinc chloride concentration. Each point represents the egg-to-adult development time of a single animal. To more easily connect the development time data with emergence data in Figure 3 we have inverted the *y*-axes in these plots; points nearer the top of each panel reflect faster development. (A) Outbred animals derived from X-QTL replicate 9 and 10 (R9, R10) samples; Significant population-by-treatment interaction ($p < 0.0005$). (B) Semi-inbred lines derived from the R9 and R10 Control and Zinc-selected cohorts; Significant population-by-treatment interaction ($p < 10^{-25}$). (C) Outbred animals generated in an analogous fashion to our X-QTL design; No significant population-by-treatment interaction. See Supplementary Table 4 for full details of the ANOVA statistical analyses.

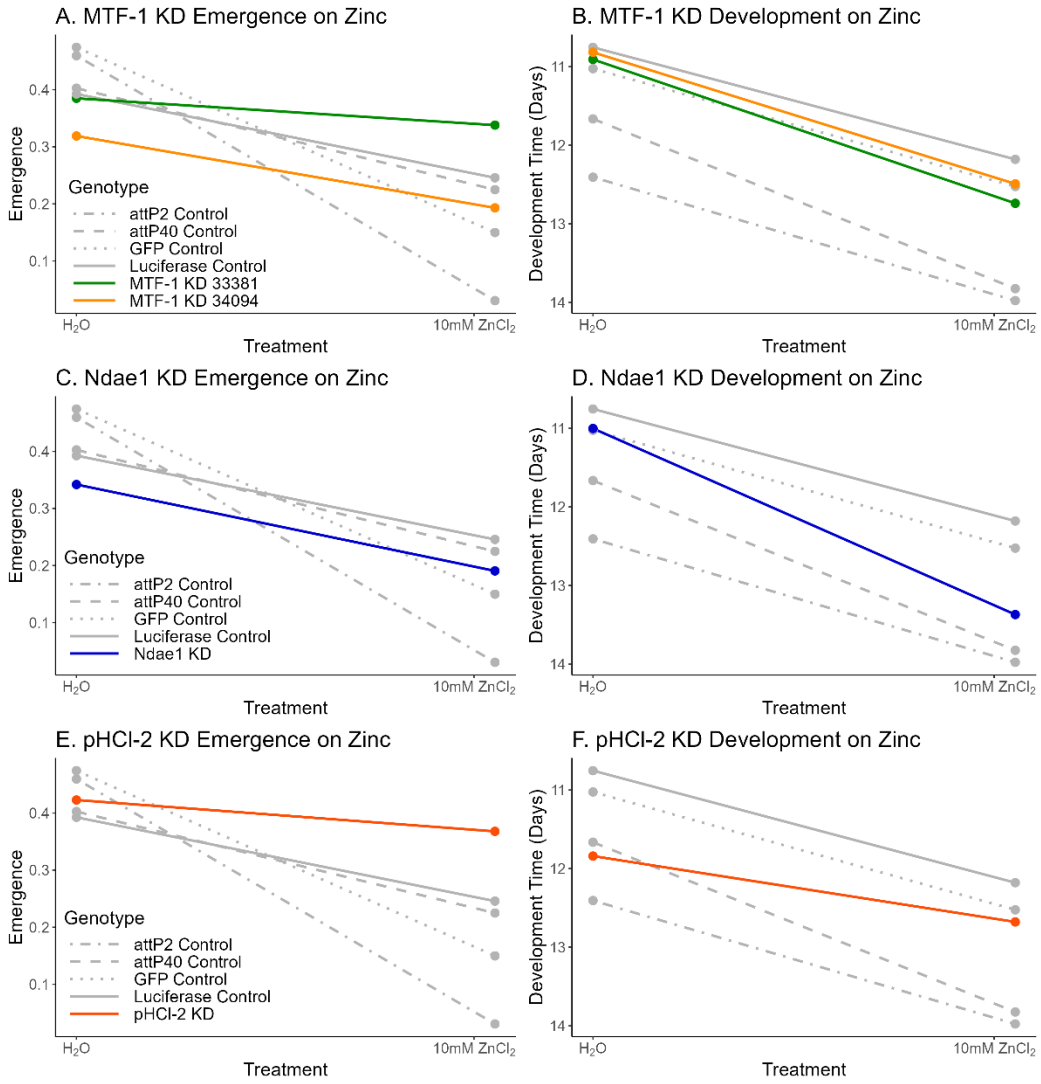

Figure 5: RNAi-based knockdowns of *MTF-1*, *Ndae1* and *pHCl-2* impact zinc resistance. Each genotype is the result of crossing a *mex1*-GAL4 strain with a strain that either carries a UAS-RNAi transgene (colored lines), or carries a control construct (gray lines). Each point represents the mean egg-to-adult emergence or development time for a given genotype for a given treatment. Confidence intervals around means were omitted for clarity, and to more easily focus on the differences in slopes between RNAi and control genotypes, which represent the genotype-by-treatment factor of interest (Supplementary Figure 4 does depict confidence intervals). Note the inverted *y*-axis used for the development time (right) panels; This was done such that a visibly negative slope for both emergence *and* development time yields the same inference; zinc treatment leads to a worse outcome (reduced emergence or longer development time.) *MTF-1* is an RNAi "hit" for emergence (panel A); knockdown using the 33381 transgene increases emergence relative to controls, as evidenced by a flatter slope. *Ndae1* is an RNAi "hit" for development time (panel D); knockdown increases developmental delay in zinc conditions as shown by a greater slope. *pHCl-2* is an RNAi "hit" for both emergence and development time (panels E and F); knockdown both increases emergence and reduces developmental delay, as evidenced by flatter slopes in both panels. See Table 2 and Supplementary Table 6 for statistical tests.